J Physiol 587.14 (2009) pp 3473–3491

Divergent regulation of GIRK1 and GIRK2 subunits of the neuronal G protein gated K^+ channel by $G\alpha_i^{GDP}$ and $G\beta\gamma$

Moran Rubinstein[1], Sagit Peleg[1], Shai Berlin[1], Dovrat Brass[1], Tal Keren-Raifman[1], Carmen W. Dessauer[2], Tatiana Ivanina[1] and Nathan Dascal[1]

[1]*Department of Physiology and Pharmacology, Sackler School of Medicine, Tel Aviv University, Tel Aviv 69978, Israel*
[2]*Department of Integrative Biology and Pharmacology, University of Texas – Houston Medical School, Houston, TX 77030, USA*

G protein activated K^+ channels (GIRK, Kir3) are switched on by direct binding of $G\beta\gamma$ following activation of $G_{i/o}$ proteins via G protein-coupled receptors (GPCRs). Although $G\alpha_i$ subunits do not activate GIRKs, they interact with the channels and regulate the gating pattern of the neuronal heterotetrameric GIRK1/2 channel (composed of GIRK1 and GIRK2 subunits) expressed in *Xenopus* oocytes. Coexpressed $G\alpha_{i3}$ decreases the basal activity (I_{basal}) and increases the extent of activation by purified or coexpressed $G\beta\gamma$. Here we show that this regulation is exerted by the 'inactive' GDP-bound $G\alpha_{i3}^{GDP}$ and involves the formation of $G\alpha_{i3}\beta\gamma$ heterotrimers, by a mechanism distinct from mere sequestration of $G\beta\gamma$ 'away' from the channel. The regulation of basal and $G\beta\gamma$-evoked current was produced by the 'constitutively inactive' mutant of $G\alpha_{i3}$, $G\alpha_{i3}$G203A, which strongly binds $G\beta\gamma$, but not by the 'constitutively active' mutant, $G\alpha_{i3}$Q204L, or by $G\beta\gamma$-scavenging proteins. Furthermore, regulation by $G\alpha_{i3}$G203A was unique to the GIRK1 subunit; it was not observed in homomeric GIRK2 channels. *In vitro* protein interaction experiments showed that purified $G\beta\gamma$ enhanced the binding of $G\alpha_{i3}^{GDP}$ to the cytosolic domain of GIRK1, but not GIRK2. Homomeric GIRK2 channels behaved as a 'classical' $G\beta\gamma$ effector, showing low I_{basal} and strong $G\beta\gamma$-dependent activation. Expression of $G\alpha_{i3}$G203A did not affect either I_{basal} or $G\beta\gamma$-induced activation. In contrast, homomeric GIRK1* (a pore mutant able to form functional homomeric channels) exhibited large I_{basal} and was poorly activated by $G\beta\gamma$. Expression of $G\alpha_{i3}^{GDP}$ reduced I_{basal} and restored the ability of $G\beta\gamma$ to activate GIRK1*, like in GIRK1/2. Transferring the unique distal segment of the C terminus of GIRK1 to GIRK2 rendered the latter functionally similar to GIRK1*. These results demonstrate that GIRK1 containing channels are regulated by both $G\alpha_{i3}^{GDP}$ and $G\beta\gamma$, while GIRK2 is a $G\beta\gamma$-effector insensitive to $G\alpha_{i3}^{GDP}$.

(Received 30 March 2009; accepted after revision 19 May 2009; first published online 26 May 2009)
Corresponding authors M. Rubinstein and N. Dascal: Department of Physiology and Pharmacology, Sackler School of Medicine, Tel Aviv University, Ramat Aviv 69978, Israel. Email: moranrub@post.tau.ac.il and dascaln@post.tau.ac.il

Abbreviations CT, C-terminus; GPCR, G protein-coupled receptor; GST, glutathione-S-transferase; HA, hemagglutinin; NT, N-terminus; PM, plasma membrane; YFP, yellow fluorescent protein; wt, wild-type.

G protein activated K^+ channels (GIRK, Kir3) mediate postsynaptic inhibitory effects of many neurotransmitters in the heart and brain. GIRK channels are switched on by direct binding of $G\beta\gamma$ following activation of $G_{i/o}$ proteins via numerous G protein coupled receptors (GPCRs) (Logothetis *et al.* 1987; Wickman & Clapham, 1995; Dascal, 2001). Although GIRK is not considered an effector for $G\alpha$ subunits, fast and specific channel activation was attributed to formation of GPCR–$G\alpha_i\beta\gamma$–GIRK signalling complexes (Huang *et al.* 1995; Slesinger *et al.* 1995; Leaney *et al.* 2000; Peleg *et al.* 2002; Ivanina *et al.* 2004). GIRK subunits interact with $G\beta\gamma$ subunits *in vitro* (Huang *et al.* 1995; Kunkel & Peralta, 1995; Huang *et al.* 1997; Ivanina *et al.* 2003; Finley *et al.* 2004) and in living cells before and after agonist activation (Rebois *et al.* 2006; Riven *et al.* 2006). Cytosolic GIRK segments also bind $G\alpha_i^{GDP}$ and $G\alpha_i^{GTP\gamma S}$ *in vitro*, and GIRK channels immunoprecipitate with $G\alpha$ subunits in native brain membranes (Huang *et al.* 1995; Ivanina *et al.* 2004; Clancy *et al.* 2005), but interaction of $G\alpha$ with GIRK *in vivo* is under debate (Fowler *et al.* 2006; Rebois *et al.* 2006).

The main neuronal GIRK channel is a GIRK1/2 heterotetramer, composed of GIRK1 and GIRK2 subunits. These subunits can also co-assemble with GIRK3 to form GIRK1/3 and GIRK2/3. GIRK1/2 channels are abundant

DOI: 10.1113/jphysiol.2009.173229

in the hippocampus and the cerebellum. GIRK2 can also form functional homomeric channels, which form the majority of GIRKs in the substantia nigra (Slesinger *et al.* 1996; Inanobe *et al.* 1999; Saenz del Burgo *et al.* 2008). In hippocampal and locus coeruleus neurons, GIRKs possess a substantial basal activity (I_{basal}) (Luscher *et al.* 1997; Torrecilla *et al.* 2002; Chen & Johnston, 2005; Wiser *et al.* 2006). The mechanisms of regulation of I_{basal} and its relation to the neurotransmitter-evoked activity (I_{evoked}) are poorly understood. We have previously presented evidence that in expression systems, $G\alpha_i$ regulates GIRK gating, keeping I_{basal} low and preparing the channel for activation by 'free' $G\beta\gamma$ (Peleg *et al.* 2002; Rishal *et al.* 2005; Rubinstein *et al.* 2007). We proposed that this action was carried out by $G\alpha^{GDP}$ (classically considered as the inactive form of $G\alpha$), possibly as a heterotrimer with $G\beta\gamma$. However, the involvement of 'active' $G\alpha^{GTP}$ could not be ruled out.

Divergent subunit compositions of GIRK channels have not been systematically studied. However, subunit content appears to play a role in coupling of GIRKs to $GABA_B$ receptors (Cruz *et al.* 2004; Fowler *et al.* 2006) and GIRK1/3 was shown to have higher affinity to $G\beta\gamma$ compared to GIRK2/3 (Jelacic *et al.* 2000). When expressed as homomers, GIRK1 ($GIRK1_{F137S}$, a functional pore mutant, denoted GIRK1*) displayed low conductance compared to GIRK1/2 or GIRK1/4, and long bursts of activity (Chan *et al.* 1996; Vivaudou *et al.* 1997), whereas GIRK2 showed higher conductance than GIRK1* but low open probability with brief, flickery openings (Yi *et al.* 2001). *In vitro* studies suggested a smaller $G\beta\gamma$ and $G\alpha$ binding surface in N and C termini of GIRK2 compared with GIRK1 (Ivanina *et al.* 2003; Ivanina *et al.* 2004). Yet, no definite differences in $G\beta\gamma$ or $G\alpha_i$ regulation of GIRK1 and GIRK2 have been reported so far.

We explored the mechanisms of regulation of GIRK channels (heteromeric GIRK1/2 channel as well as homomeric GIRK1 and GIRK2 channels) by $G\alpha_i$ and $G\beta\gamma$ using *in vitro* protein interaction assay and functional assays in *Xenopus* oocytes. To definitely distinguish between the effects of 'inactive' $G\alpha^{GDP}$ and 'active' $G\alpha^{GTP}$, we utilized 'constitutively inactive' and 'constitutively active' $G\alpha_{i3}$ mutants. We demonstrate a profound regulation of the heteromeric GIRK1/2 and the homomeric GIRK1* channels by $G\alpha_{i3}{}^{GDP}$, probably in the context of the $G\alpha_i\beta\gamma$ heterotrimer. This regulation does not occur in homomeric GIRK2 channels, leading to different regulation of GIRK1 and GIRK2 by $G\beta\gamma$, and to an asymmetric regulation by $G\alpha_i\beta\gamma$ heterotrimer.

Methods

DNA constructs and mRNA

The cDNA constructs were described in previous publications (Peleg *et al.* 2002; Rishal *et al.* 2005). cDNA constructs were inserted into pGEX (for production of glutathione-S-transferase (GST) fusion proteins in *E. coli*) or into high-expression oocyte vectors containing 5′ and 3′ untranslated sequences of *Xenopus* β-globin: pGEMHE, pGEMHJ, or pBS-MXT. Rat GIRK1 (U01071), mouse GIRK2a (U11859), and human $G\alpha_{i3}$ (J03198) were used for oocytes expression and for deriving mutants, except human GIRK1* (U39195).

$G\alpha_{i3}$G203A and $G\alpha_{i3}$Q204L were produced using standard PCR-based methods and fully sequenced. The HA-(hemagglutinin)-tagged GIRK2 (Chen *et al.* 2002; Clancy *et al.* 2005) was subcloned into pBS-MXT. Yellow fluorescent protein (YFP) was fused in-frame before the N-terminus of GIRK1* or GIRK2, or after the C-terminus of GIRK2, essentially as described by Riven *et al.* (2003) and Fowler *et al.* (2006). G1NC and G2NC constructs were made by PCR; the transmembrane segments (GIRK1 a.a 85–184; GIRK2 a.a 96–193) were deleted, and N-terminus and C-terminus (NT and CT, respectively) were connected by a linker encoding amino acids QSTASQST in G1NC and KL in G2NC. The $G2_{CT}G1$ chimera ($GIRK2_{HA(a.a1-381)}GIRK1_{(a.a371-501)}$) was constructed using PCR followed by blunt end ligation. All PCR products were fully sequenced. RNAs were synthesized *in vitro* as described (Kanevsky & Dascal, 2006) and injected into oocytes at 0.2–20 ng per oocyte. To prevent the formation of GIRK1*/5 heterotetramers, we injected antisense targeted against the oocytes' endogenous GIRK5 subunits (Hedin *et al.* 1996) when studying GIRK1*.

Xenopus oocytes preparation and electrophysiology

Experiments were approved by the Tel Aviv University Institutional Animal Care and Use Committee (permit no. 11-05-064). Briefly, female frogs, maintained at $20 \pm 2^{\circ}$C on an 11 h light–13 h dark cycle, were anaesthetized in a 0.15% solution of procaine methanesulphonate (MS222), and portions of ovary were removed through a small incision on the abdomen. The incision was sutured, and the animal was returned to a separate tank until it had fully recovered from the anaesthesia, and afterwards was returned to a large tank, together with the other post-operational animals. The animals did not show any signs of postoperational distress and were allowed to recover for at least 8 weeks until the next surgery. Following the final collection of oocytes, the frogs were killed by decapitation and double pithing while under anaesthesia. Oocytes were defolliculated by collagenase, injected with RNA (Peleg *et al.* 2002) and incubated for 3 days (whole cell studies) or 2–4 days (patch clamp) at 20–22°C in ND96 solution (low K^+) containing, in mM: 96 NaCl, 2 KCl, 1 $MgCl_2$, 1 $CaCl_2$, 5 Hepes, pH 7.5, supplemented with 2.5 mM sodium pyruvate, 100 μg ml^{-1} streptomycin and

62.75 μg ml^{-1} penicillin (or 50 μg ml^{-1} gentamycine). Whole-cell GIRK currents were measured using standard two-electrode voltage clamp procedures (Rubinstein *et al.* 2007) at 20–22°C, in high K^+ solutions (24 mM K^+ for GIRK1*, and 24, 48 or 96 mM for GIRK2, as indicated). K^+ solutions at 24 and 48 mM were obtained by mixing ND96 with a 96 mM K^+ solution containing, in mM: 96 KCl, 2 NaCl, 1 $CaCl_2$, 1 $MgCl_2$, 5 Hepes, pH 7.5. Acetylcholine (ACh) was used at 10 μM. Whole cell currents produced by the expression of untagged or YFP-tagged homomeric GIRK1* were similar in amplitude and in regulation by $G\beta\gamma$, and the data were pooled. The same was observed with untagged, HA- or YFP-tagged GIRK2 channels.

Patch clamp experiments were performed as described (Peleg *et al.* 2002). Data acquisition and analysis were done using pCLAMP software (Molecular Devices, Sunnyvale, CA, USA) as described (Peleg *et al.* 2002). Currents were recorded at a holding potential of −80 mV, sampled at 10 kHz and filtered at 2 kHz. Patch pipettes had resistances of 1.2–2.5 MΩ. After seal formation, the patches were excised and exposed to air to prevent the formation of closed membrane vesicles at the tip. Stock solution (10 μM) of the purified $G\beta_1\gamma_2$ protein was diluted into 50 μl of the bath solution (final concentration of 20–40 nM as indicated), added to the 500 μl solution in the bath, and stirred. For patch recordings of heteromeric GIRK1/2 channels, the pipette solution contained, in mM: 144 KCl, 2 NaCl, 1 $MgCl_2$, 1 $CaCl_2$, 1 $GdCl_3$, 10 Hepes/KOH, pH 7.5. Bath solution contained, in mM: 130 KCl, 2 $MgCl_2$, 1 EGTA, 2 Mg-ATP, and 10 Hepes/KOH, pH 7.5. Measurements of homomeric channels were made with a pipette solution that contained, in mM: 146 KCl, 2 NaCl, 1 $MgCl_2$, 1 $CaCl_2$, 1 $GdCl_3$, 10 Hepes/KOH, pH 7.5. Bath solution contained, in mM: 146 KCl, 6 NaCl, 2 $MgCl_2$, 1 EGTA, 2 Mg-ATP, 10 Hepes/KOH, pH 7.5. (The presence of NaCl was found essential to prevent strong rundown of GIRK1* channels in excised patches.) $GdCl_3$ completely inhibited the stretch-activated channels. For the comparison of channel activity in excised patches *vs.* cell attached patches, currents were also corrected for changes in the single channel amplitude, *i*. For GIRK1/2, *i* was taken as 2.4 pA in cell-attached and 2.2 nA in excised patches (authors' unpublished observations). For GIRK1*, *i* was 1.24 ± 0.03 pA in cell-attached mode and 1.06 ± 0.03 pA in excised mode. For $GIRK2_{HA}$, *i* was 1.4 ± 0.07 pA and 1.03 ± 0.08 pA in cell attached and excised mode, respectively. For GIRK2, *i* was 1.74 ± 0.05 pA and 1.49 ± 0.05 pA in cell attached and excised mode, respectively.

HEK293 transfection and electrophysiology

HEK293 cells were cultured in Dulbecco's modified Eagle's medium (DMEM) supplemented with 2 mM glutamine, 10% fetal calf serum, 100 units ml^{-1} penicillin-G sodium and 100 μg ml^{-1} streptomycin sulfate in an atmosphere of 95% air–5% CO_2 at 37°C. Cells were transfected using the Fugene^{R}6 Transfection Reagent (Roche Applied Science, USA), in a 24-well dish, with cDNAs of GIRK1 and GIRK2 (0.2–0.6 μg), m2R (0.5 μg), and (when designed) of $G\alpha_{i3}$ (0.15–0.3 μg), m-phosducin (0.2 μg), $G\beta_1$ and $G\gamma_2$ (0.2 μg each). Total DNA concentration was adjusted to 2.1 μg per 1.5 cm well by adding empty pcDNA3 vector DNA. The CD8 reporter gene system was used to visualize transfected cells (0.5 μg DNA per well). Beads coated with anti-CD8-antibodies were purchased from Invitrogen.

Whole cell recordings were performed at 21–23°C. Patch pipette solution contained, in mM: 130 KCl, 1 $MgCl_2$, 5 EGTA, 3 MgATP, 10 Hepes. Low-K bath solution contained, in mM: 140 NaCl, 4 KCl, 1.8 $CaCl_2$, 1.2 $MgCl_2$, 11 glucose, 2 $CdCl_2$, 5.5 Hepes. High-K bath solution contained 90 mM KCl and 54 mM NaCl; the rest was as in low-K solution. The osmolarity of intracellular and extracellular solutions was adjusted to 290 and 310 mosmol l^{-1} respectively, with sucrose; pH was 7.4–7.6. Patch clamp was done using an Axopatch 200B (Molecular Devices). Data acquisition and analysis were done using pCLAMP software (Molecular Devices).

Biochemistry

GST-fused $G\alpha_{i3}$ (GST-$G\alpha_{i3}$) was purified as described (Rishal *et al.* 2003). [^{35}S]Methionine-labelled G1NC ($G1N_{1-84}C_{183-501}$) and G2NC ($G2N_{1-95}C_{194-414}$) proteins were synthesized in rabbit reticulocyte lysate (Promega Corp., Madison, WI, USA). For pull down experiments, 3 μg of GST-$G\alpha_{i3}$ was incubated at 30°C with 30 μM of GDP for 30 min in 50 μl of a high-K^+ binding buffer (Rishal *et al.* 2003) containing 0.01% Lubrol. Purified recombinant $G\beta_1\gamma_2$ (3 μg, wild-type or His_6-tagged) or vehicle was added for another 30 min. Then, 5 μl of reticulocyte lysate containing [^{35}S]methionine-labelled G1NC or G2NC was added, the total reaction volume was brought to 300 μl, 5 μl was removed and used to measure the loaded protein ('input'), and the incubation continued for 1 h at room temperature. Binding to glutathione-Sepharose beads and elution with 15 mM glutathione were done as described (Rishal *et al.* 2003). The eluted proteins were separated on 12% polyacrylamide-SDS gels. The radioactive signals from protein bands of the gels were imaged using PhosphorImager and the software ImageQuaNT (Molecular Dynamics). Western blots were performed using standard procedures, using $G\beta$ antibody (Santa Cruz Biotechnology, Inc., Santa Cruz, c.a., USA) and ECL reagents (Pierce Biotechnology, Inc., Rockford, IL, USA).

Imaging and immunocytochemistry

Imaging of proteins in the plasma membrane (PM) was performed either in giant PM patches or in whole oocytes.

Imaging of homomeric GIRK1* in PM was performed using N or C terminally YFP-labelled channels in whole oocytes (Fig. 5*A* and Supplemental Fig. 2*A*), or immunolabelling of untagged channels in giant excised PM patches using GIRK1 antibody (Fig. 6*A*). GIRK2 expression was monitored in intact oocytes with either C terminally labelled YFP channel (Supplemental Fig. 2*A*), or $GIRK2_{HA}$ channels with an extracellular HA tag (Figs 5*A* and 8*A* and *C*) or giant PM patches using GIRK2 antibody (Fig. 8*A*). Immunocytochemistry in giant PM patches was done essentially as described (Singer-Lahat *et al.* 2000; Peleg *et al.* 2002). In brief, the vitelline membrane was peeled off and the oocytes were placed on plastic coverslips (Thermanox plastic coverslip, Nunc, Naperville, IL, USA). After sticking to the coverslip, the oocyte was removed by washing with a strong jet of solution. Pieces of membrane attached to the coverslip, with their cytosolic leaflet surface exposed to the external solution, were washed until the membrane patch became transparent. Following fixation for 10 min in 1% formaldehyde, the membranes were washed three times with 5% skim milk dissolved in phosphate-buffered saline (PBS). Blocking of non-specific binding sites was done with donkey immunoglobulin G (IgG, whole molecule, 1/400, Jackson ImmunoResearch Laboratories, Inc., West Grove, PA, USA) for 30 min. Each coverslip was incubated for 1 h with antibodies against GIRK1 or GIRK2 (Alomone Labs, Jerusalem, Israel). Residual antibody was washed out with 5% skim milk 3 times, 5 min each. This was followed by a 30 min incubation with secondary antibody (Cy3 donkey anti-rabbit IgG, 1 : 400, Jackson ImmunoResearch Laboratories). Free secondary antibody was then washed out with PBS 3 times, 5 min each in darkness and the coverslips were mounted on a glass slide. The fluorescent labelling was examined by a confocal laser scanning microscope (LSM 510 Meta, Zeiss, Germany) with 20× or 5× objective lens. Cy3 was excited at 514 nm and the emitted light was collected between 540 and 615 nm using the spectral mode of the Zeiss 510 Meta (beam splitter HFT 405/514/633).

Imaging of whole oocytes was done using external HA tag ($GIRK2_{HA}$, $G2_{CT}G1$) (Kanevsky & Dascal, 2006) or YFP (YFP labelled GIRK1* or GIRK2). To visualize the HA tag, whole oocytes expressing $GIRK2_{HA}$ or $G2_{CT}G1$ were fixated in 4% formaldehyde (from 37% stock) in Ca^{2+}-free ND96 solution for 30 min. Blocking of non-specific binding sites was done by 5% skim milk for 1 h in Ca^{2+}-free ND96. Then the oocytes were incubated for 1 h with the mouse monoclonal anti-HA antibody (Santa Cruz Biotechnology), diluted 1 : 400 in 2.5% skim milk. Residual antibody was washed out with 2.5% skim milk 3 times, 5 min each. This was followed by 1 h incubation with the secondary antibody (Alexa Fluor 488 conjugated, 1 : 400, Molecular Probes/Invitrogen) in dark. Free secondary antibody was then washed out with Ca^{2+}-free ND96. Oocytes were placed in a chamber with a transparent bottom, and fluorescence imaging was performed with LSM 510 (×20 objective, zoom = 2, pinhole 3 Airy units). Alexa was excited at 488 nm, and the emitted light was collected in the wavelength interval of 508–615 nm in spectral mode (with HFT 405/488 beam splitter).

Imaging of YFP labelled GIRK1* and GIRK2 channels was performed with LSM 510 (×20 objective, zoom = 2, pinhole 3 Airy units). YFP was excited at 514 nm, and the emitted light was collected in the wavelength interval of 524–609 nm in spectral mode (with HFT 405/514/633 beam splitter).

All images were obtained from optical slices from the animal hemisphere close to the oocyte's equator. Quantification of all the images was done using Zeiss LSM software. The intensity of fluorescence in the PM was measured by averaging the signal obtained from three standard regions of interest. Net fluorescence intensity per unit area was obtained by subtracting the background signal measured in uninjected oocytes. In all confocal imaging procedures, care was taken to completely avoid saturation of the signal. In each experiment, all oocytes from the different groups were studied using constant LSM settings.

Data analysis, presentation and statistics

Relative activation by agonist, R_a, was calculated in each cell as I_{total}/I_{basal}, where $I_{total} = I_{basal} + I_{ACh}$. Thus, $R_a = I_{total}/I_{basal} = (I_{ACh} + I_{basal})/I_{basal} = (I_{ACh}/I_{basal}) + 1$. Similarly, the extent of $G\beta\gamma$ activation, $R_{\beta\gamma}$, was defined as $R_{\beta\gamma} = I_{\beta\gamma}/I_{basal}$, where $I_{\beta\gamma}$ is the total $G\beta\gamma$-dependent current. The better the activation by $G\beta\gamma$, the greater is $R_{\beta\gamma}$; $R_{\beta\gamma} = 1$ when there is no effect of $G\beta\gamma$. In patch clamp experiments, I_{basal} was measured in a cell-attached mode before excision, and $I_{\beta\gamma}$ in the same patch after excision and addition of purified $G\beta\gamma$ (Figs 3, 7 and 9). In whole cells, $I_{\beta\gamma}$ is the total GIRK current in a cell expressing $G\beta\gamma$, and I_{basal} is the average GIRK current in oocytes of the same batch expressing GIRK alone (Rubinstein *et al.* 2007). These definitions are essentially the same as the ones used previously ($R_a = I_{ACh}/I_{basal}$; $R_{\beta\gamma} = I_{\beta\gamma}/I_{basal} - 1$) (Peleg *et al.* 2002; Rubinstein *et al.* 2007) except for the addition of a constant number, 1. The change in definition was motivated by the desire to avoid division by very small numbers during normalization to (division by) R_a or $R_{\beta\gamma}$ of the 'GIRK only' groups. Indeed, R_a and $R_{\beta\gamma}$ calculated according to the previous definition (Rubinstein *et al.* 2007) were often close to zero in these cells at high expression levels of GIRK1/2 or GIRK1*, when the activation by ACh or by $G\beta\gamma$ was weak.

Results are shown as means ± S.E.M. When summarizing several experiments, in order to minimize batch-to-batch

variations and to enhance the accuracy of the statistical analysis, whole-cell GIRK currents were normalized, in each oocyte, to the average GIRK current of the control group (GIRK alone) of the same experiment (Sharon *et al.* 1997). Two group comparisons were done using Student's two-tailed *t*-test. Multiple group comparison was done using one-way analysis of variance (ANOVA) followed by Tukey's, Student–Neumann–Keuls or Dunnet's test. Correlations between two parameters were examined using Spearman's test.

Results

$G\alpha_{i3}$ regulates GIRK1/2 gating in HEK 293 cells, like in oocytes

We have previously observed that the I_{basal} of GIRK1/2 increased disproportionally as the channel expression level was increased, whereas activation by agonist or $G\beta\gamma$ became weaker; there is a negative correlation between I_{basal} and the extent of activation by agonist (R_a) or by $G\beta\gamma$ ($R_{\beta\gamma}$). This abnormal gating was corrected by coexpressed $G\alpha_{i3}$ which reduced I_{basal}, increased R_a and $R_{\beta\gamma}$, but did not reduce the total $G\beta\gamma$-dependent current (basal + evoked), I_{total}, as if the presence of $G\alpha_{i3}$ prepares ('primes') the channel for activation by $G\beta\gamma$ (Peleg *et al.* 2002; Rubinstein *et al.* 2007). The enhancement of agonist-evoked current by coexpressed $G\alpha_i$ appeared self-evident (Vivaudou *et al.* 1997; He *et al.* 1999) (free $G\beta\gamma$ is sequestered by $G\alpha_i{}^{GDP}$ but then released after activation of GPCR). However, the enhancement of activation induced by added or coexpressed $G\beta\gamma$ could not be fully explained by a mechanism in which $G\alpha$ reduces I_{basal} by 'sequestering $G\beta\gamma$ away' from GIRK (Rusinova *et al.* 2007), suggesting a more complex mechanism, where the GIRK channel may be regulated by $G\alpha_{i3}{}^{GDP}$ (Peleg *et al.* 2002).

The aforementioned hallmarks of $G\alpha_i$ regulation have been observed so far only in *Xenopus* oocytes, which are believed to have relatively high levels of $G\beta\gamma$ that help to maintain the meiotic arrest (Sheng *et al.* 2001; Evaul *et al.* 2007). Therefore, it was important to show that regulation by $G\alpha_i$ does not arise from some unusual properties of *Xenopus* oocytes. To this end, we transiently transfected HEK 293 cells with GIRK1, GIRK2 and the muscarinic 2 receptor (m2R). Evoked currents were elicited by acetylcholine (ACh) or by coexpression of $G\beta\gamma$. In general, R_a and $R_{\beta\gamma}$ were somewhat higher in HEK 293 cells than in oocytes, corroborating higher basal $G\beta\gamma$ levels in the oocytes. Despite this quantitative difference, the fundamental hallmarks of $G\alpha_{i3}$ regulation were as in *Xenopus* oocytes (Fig. 1). There was a strong negative correlation between I_{basal} (taken as the indicator of expression level) and R_a or $R_{\beta\gamma}$; expression of $G\alpha_{i3}$ restored the low I_{basal} and high activation by agonist and $G\beta\gamma$, whereas the membrane-attached $G\beta\gamma$ scavenger protein m-phosducin (Rishal *et al.* 2005; Rubinstein *et al.* 2007) diminished both I_{basal} and the evoked currents. For further functional assays we used *Xenopus* oocytes, where protein expression levels can be accurately controlled and monitored.

'Constitutively inactive' mutant of $G\alpha_{i3}$, $G\alpha_{i3}$GA, regulates the basal activity and $G\beta\gamma$ activation of heteromeric GIRK1/2

We envisaged that coexpressed $G\alpha_{i3}$ regulated GIRK1/2 in its GDP-bound form, but the involvement of $G\alpha_i{}^{GTP}$ could not be excluded (Peleg *et al.* 2002; Rubinstein *et al.* 2007). In order to decisively distinguish between effects of $G\alpha_i{}^{GDP}$ and $G\alpha_i{}^{GTP}$, we used two mutants

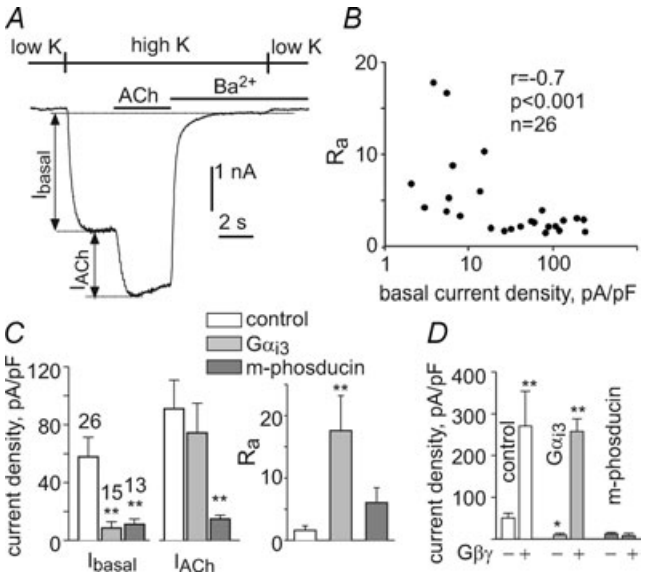

Figure 1. Regulation of GIRK1/2 channels expressed in HEK293 cells

A, HEK 293 cells were transiently transfected with GIRK1, GIRK2 and the muscarinic 2 receptor (m2R). GIRK1/2 currents were studied using whole-cell voltage clamp at −80 mV. Switching from a physiological low-K^+ solution to a high-K^+ solution (90 mM K^+) revealed GIRK1/2 I_{basal}. Addition of the agonist acetylcholine (ACh; 10 μM) evoked I_{ACh}. Ba^{2+} at 5 mM was then added to inhibit GIRK currents, to calculate the net I_{basal} and I_{ACh}. *B*, R_a is negatively correlated with I_{basal} (to account for differences in HEK cell size, we used current densities (in pA pF^{-1}) in all calculations rather than net currents). Correlation coefficient (*r*), statistical significance (*P*), and number of measurements (*n*) are indicated. R_a in HEK cells was usually greater than in *Xenopus* oocytes, up to 18 (in the oocytes it is usually below 5), corroborating higher basal $G\beta\gamma$ levels in the oocytes. *C*, coexpression of $G\alpha_{i3}$ and m-phosducin reduced I_{basal} similarly, but only $G\alpha_{i3}$ enhanced the relative activation by ACh, R_a. *D*, coexpressed $G\alpha_{i3}$, but not m-phosducin, improves activation of GIRK1/2 by expressed $G\beta\gamma$. $n = 3$–7 cells in each group. The extent of direct activation by $G\beta\gamma$ ($R_{\beta\gamma}$), calculated here as the ratio of average currents in cells expressing $G\beta\gamma$ to those without $G\beta\gamma$, was 5.4 for GIRK alone, 26 in the presence of $G\alpha_{i3}$, and 0.68 in the presence of m-phosducin. $^*P < 0.05$; $^{**}P < 0.01$ compared to control by ANOVA.

of Gα. One is the 'constitutively active' $G\alpha_{i3}$Q204L ($G\alpha_{i3}$QL), which poorly hydrolyses GTP, has a reduced affinity for Gβγ and regulates effectors of $G\alpha_i^{GTP}$ in a GPCR-independent manner (Masters *et al.* 1989). The second one is the 'constitutively inactive' $G\alpha_{i3}$G203A ($G\alpha_{i3}$GA), which strongly binds Gβγ (Ogier-Denis *et al.* 1996). GαGA mutants can bind GTP but do not regulate known effectors of $G\alpha^{GTP}$ (Lee *et al.* 1992).

Upon injection of a standard dose of 1–2 ng RNA per oocyte, $G\alpha_{i3}$-wild-type (wt) and its two mutants were expressed in the PM at similar levels, more than 4-fold over the endogenous $G\alpha_{i/o}$, with no effect on GIRK1/2 expression level (data not shown). As described in other cells (Fishburn *et al.* 1999; Evanko *et al.* 2000), Gα and Gβγ mutually affected each other's PM levels. Expression of Gβγ further increased the PM levels of expressed $G\alpha_{i3}$, $G\alpha_{i3}$GA and $G\alpha_{i3}$QL by ∼ 35%, and expression of $G\alpha_{i3}$ or $G\alpha_{i3}$GA increased the PM level of coexpressed Gβγ by about 50%, whereas $G\alpha_{i3}$QL was without effect (data not shown).

Since both Gα mutants disrupt the G protein cycle, we activated GIRK by coexpressed Gβγ (in whole oocytes; see Reuveny *et al*. 1994; Rubinstein *et al*. 2007) or by purified Gβγ (in excised patches), thus bypassing the GPCR. Here, the channels are activated by the externally added Gβγ, without the $G\alpha_i\beta\gamma$ heterotrimer dissociation and without formation of $G\alpha_i^{GTP}$. As controls for $G\alpha_{i3}$ mutants, we expressed two genetically engineered Gβγ scavengers that accumulate at the PM because they are N-terminally myristoylated, like $G\alpha_i$, and act as 'sinks' for Gβγ: m-phosducin and m-cβARK (a modified C-terminal part of β-adrenergic receptor kinase 1) (Rishal *et al.* 2005). We found that m-phosducin moderately reduced the total amount of detectable coexpressed Gβγ in the PM, strengthening the notion of its being a strong Gβγ sink, whereas cβARK had no effect (data not shown).

With the high GIRK1/2 levels used, I_{basal} was large ($14 \pm 2\ \mu$A, $n = 31$) and the expression of Gβγ produced little additional activation (examples in Fig. 2*A*, summarized in Fig. 2*B*); the average relative activation by Gβγ ($R_{\beta\gamma}$) in this series of experiments was 1.4 ± 0.1 (Fig. 2*C*). $G\alpha_{i3}$GA, m-phosducin and m-cβARK reduced I_{basal}, whereas $G\alpha_{i3}$QL did not alter I_{basal} (Fig. 2*B*). We titrated the RNA dosage of $G\alpha_{i3}$GA, phosducin and m-cβARK to attain a comparable 72–82% reduction in I_{basal} (at RNA doses of 2, 5 and 10 ng RNA per oocyte, respectively; data not shown) and used these doses in experiments of Fig. 2. Despite the similar decrease in I_{basal}, the three proteins had disparate effects on GIRK1/2's activation by Gβγ. $G\alpha_{i3}$GA did not reduce the total Gβγ-dependent current, $I_{\beta\gamma}$, and significantly enhanced $R_{\beta\gamma}$ (by 6.15 ± 0.83-fold compared to control; $n = 25$). In contrast, c-βARK reduced $I_{\beta\gamma}$ by ∼75%, almost completely preventing channel activation by the coexpressed Gβγ (Fig. 2*B*). Accordingly, in the presence of m-cβARK, $R_{\beta\gamma}$ was the lowest among all conditions, only 1.21 ± 0.1 (compare with 8.6 ± 1.2 with $G\alpha_{i3}$GA; Fig. 2*C*). m-Phosducin slightly increased $R_{\beta\gamma}$, but significantly less than $G\alpha_{i3}$GA. Furthermore, m-phosducin also significantly reduced $I_{\beta\gamma}$, in contrast to $G\alpha_{i3}$GA (Fig. 2*B* and *C*). The disparate effects of $G\alpha_{i3}$GA and the two Gβγ scavengers confirm that the effect of $G\alpha_{i3}$GA is distinct from simple Gβγ sequestration away from GIRK.

We next studied GIRK1/2 regulation by Gα mutants in excised patches, which has the advantage of strictly

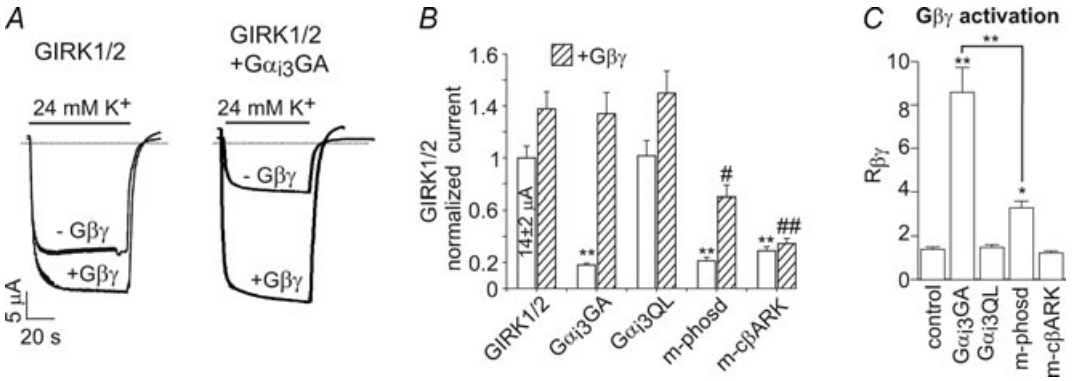

Figure 2. $G\alpha_{i3}$GA improves GIRK1/2 activation by coexpressed Gβγ in whole oocytes
A, examples of GIRK1/2 currents in four individual oocytes of one batch expressing GIRK1/2 with or without Gβγ (left panel), or GIRK1/2 with 2 ng $G\alpha_{i3}$GA, with or without Gβγ (right panel). Five nanograms of RNA of $G\beta_1$ and 1 ng RNA of $G\gamma_2$ were injected. Zero current is indicated by dashed lines (note that an outward I_{basal} is present in the low, 2 mM K^+ solution). *B*, the effects of coexpression of $G\alpha_{i3}$GA or $G\alpha_{i3}$QL (2 ng RNA), m-phosducin (5–10 ng) and m-cβARK (5 ng) on basal and Gβγ-induced whole-cell currents. (The data with 5 and 10 ng m-phosducin were pooled as they produced quite similar effects.) $^{**}P < 0.01$ compared to control I_{basal}; $\#P < 0.05$ or $\#\#P < 0.01$ compared with control $I_{\beta\gamma}$. *C*, $R_{\beta\gamma}$ of the experiments summarized in *B*. $^{*}P < 0.05$ and $^{**}P < 0.01$ against control or between indicated groups. $n = 8$–31.

controlling the concentration of added $G\beta\gamma$ and measuring I_{basal} and $I_{\beta\gamma}$ in the same oocyte. GIRK1/2 was expressed alone or with $G\alpha_{i3}$GA or $G\alpha_{i3}$QL. After 1–3 min of cell-attached (c.a.) recording of I_{basal}, patches were excised. The activity declined, reaching a new steady level within 0.5–2 min (Peleg *et al.* 2002). Approximately 3 min after excision, purified $G\beta_1\gamma_2$ (20 nM) was added to the bath solution to activate the channel (Fig. 3*A*). Coexpressed $G\alpha_{i3}$GA strongly reduced I_{basal} but significantly enhanced $R_{\beta\gamma}$ compared to control group (Fig. 3*B*). $G\alpha_{i3}$QL caused a mild reduction in I_{basal} ($P > 0.05$) and no significant changes in $R_{\beta\gamma}$. $I_{\beta\gamma}$ was unchanged by either $G\alpha_{i3}$GA or $G\alpha_{i3}$QL. This result (and also the similar result with GIRK1*, Fig. 7) rules out the possibility that the enhanced activation observed with $G\alpha_{i3}$GA coexpression was due to $G\alpha$-dependent changes in the level of $G\beta\gamma$, as could potentially happen with coexpressed proteins in whole cell experiments. The effect of $G\alpha_{i3}$GA was in sharp contrast to that of m-cβARK, which greatly reduced $G\beta\gamma$-induced activation of GIRK1/2 in excised patches (Peleg *et al.* 2002). Thus, in excised patches $G\alpha_{i3}$GA, but not $G\alpha_{i3}$QL, regulates the channel basal activity, and improves the relative activation by added $G\beta\gamma$.

To summarize, $G\alpha_{i3}$GA has a unique effect on GIRK1/2 gating: similarly to $G\alpha_{i3}$-wt, it reduces I_{basal}, enhances $R_{\beta\gamma}$, and does not reduce the total $I_{\beta\gamma}$. Neither the two $G\beta\gamma$ scavengers tested nor $G\alpha_{i3}$QL can reproduce these effects. We conclude that the regulation of I_{basal} and of the $G\beta\gamma$-evoked activation of GIRK1/2 is produced by the GDP-bound form of $G\alpha_{i3}$.

$G\beta\gamma$ enhances the interaction of $G\alpha_{i3}^{GDP}$ with GIRK1 but not GIRK2

We have examined the interaction of *in vitro* translated cytosolic domain of GIRK1 (a tandem of full-length N- and C-termini, G1NC, which lacks the transmembrane domain; see Fig. 4*A*) with $G\alpha_{i3}$ in the presence of purified $G\beta\gamma$. Interestingly, the binding of $G\alpha_{i3}^{GDP}$ to G1NC was enhanced in the presence of $G\beta\gamma$ (Fig. 4*C* and unpublished observations). To examine whether this phenomenon also takes place in GIRK2, we constructed a similar tandem, G2NC, encoding the full-length cytosolic domain of GIRK2 (Fig. 4*A*). The *in vitro* translated, ^{35}S-labelled G1NC and G2NC gave a single protein band each on SDS-polyacrylamide gels (Fig. 4*B* and *C*). Furthermore, both G1NC and G2NC bound $G\beta\gamma$ similarly (Fig. 4*B*). These results suggest that *in vitro* synthesized G1NC and G2NC are stable, well folded proteins.

Next, binding of the *in vitro translated* G1NC and G2NC to a GST-fused $G\alpha_{i3}$ (GST-$G\alpha_{i3}$) (Rishal *et al.* 2003) was examined in the presence of GDP, and in the presence or absence of purified $G\beta_1\gamma_2$. In the absence of $G\beta\gamma$, both G1NC and G2NC bound $G\alpha_{i3}$ (Fig. 4*C*). In the presence of $G\beta\gamma$, the binding of G1NC to GST-$G\alpha_{i3}$ was enhanced ~6-fold. In contrast, G2NC binding to GST-$G\alpha_{i3}$ was unaffected by the addition of $G\beta\gamma$ (Fig. 4*C*). These data suggest the formation of a strong complex between $G\alpha_{i3}\beta\gamma$ heterotrimers and GIRK1, but not GIRK2.

Functional differences between homomeric GIRK1 and GIRK2

The asymmetric interaction of GIRK1 and GIRK2 with $G\alpha_{i3}\beta\gamma$ suggested a different regulation of function of each subunit within the heteromeric channel. We therefore sought to investigate these differences using homomeric GIRK channels expressed in *Xenopus* oocytes. GIRK2 subunits form functional homomers, whereas GIRK1 does not. Thus, we used the $GIRK1_{F137S}$ (GIRK1*), a pore mutant of GIRK1, able to form functional channels in the plasma membrane (PM) (Vivaudou *et al.* 1997).

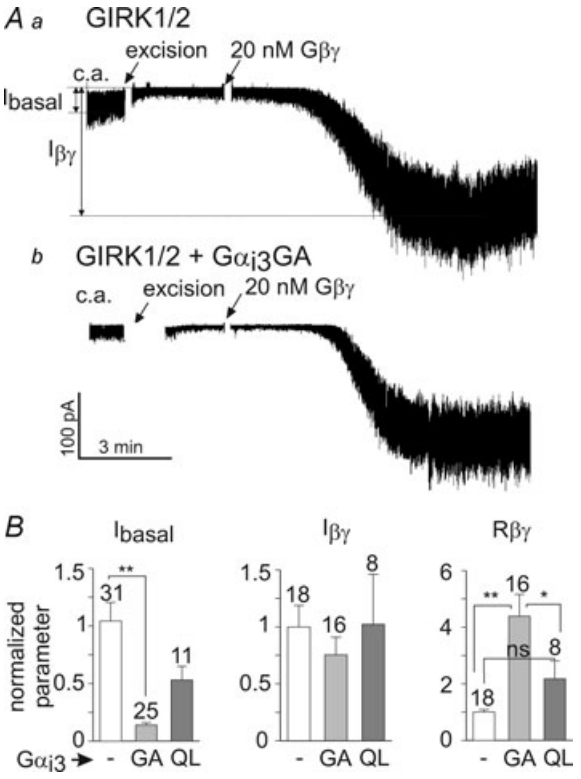

Figure 3. $G\alpha_{i3}$GA improves GIRK1/2 activation by added $G\beta\gamma$ protein in excised plasma membrane patches
A, examples of patch clamp records in oocytes expressing either GIRK1/2 alone (*a*) or with $G\alpha_{i3}$GA (*b*). RNAs at 1–2.5 ng per oocyte of GIRK1/2, $G\alpha_{i3}$GA and $G\alpha_{i3}$QL were injected. Approximate amplitudes of I_{basal} and $I_{\beta\gamma}$ are indicated for illustration in *a*; the exact values were calculated from all-points histograms (Yakubovich *et al.* 2009). *B*, summary of patch clamp experiments. In view of large batch-to-batch variability, all data (currents, $R_{\beta\gamma}$) were normalized to those of control group (GIRK1/2 alone) recorded on the same day. Number of measurements is shown above the bars. *$P < 0.05$; **$P < 0.01$.

The presence of a single mutation in the pore is not likely to affect the regulation of the channel by Gα and G$\beta\gamma$, which bind to the cytosolic segments. In support, heterotetrameric GIRK1*/GIRK2 functioned similarly to wild-type GIRK1/2, showing an excessive I_{basal} and reduced activation by agonist and G$\beta\gamma$ at high expression levels, as well as the typical regulation by Gα_{i3}GA (data not shown).

Homomeric GIRK channels were activated by ACh (via coexpressed m2R), by coexpression of G$\beta\gamma$, or by the addition of purified G$\beta\gamma$ to excised patches. For the whole cell experiments K^+ currents were measured using two electrode voltage clamp, concurrently with measurements of protein level of the channels in the PM. GIRK1* currents were always measured in 24 mM K^+, whereas most of GIRK2 recordings were done in 48 mM K^+, to allow for a better resolution of I_{basal} of the GIRK2.

Titrated expression of the two channels revealed striking differences which became especially prominent at high expression levels (10–15 ng RNA per oocyte) (see Table 1). The first difference was the magnitude of I_{basal}, which was many-fold larger in GIRK1* than GIRK2 (3 ± 0.2 μA, $n = 44$ *vs.* 0.38 ± 0.06, $n = 40$; $P < 0.001$, Fig. 4*D–F*). This occurred despite the fact that GIRK2 expression was higher compared to GIRK1* (Supplemental Fig. 2), and despite the fact that we used higher K^+ concentration in GIRK2 measurements. Moreover, I_{basal} of GIRK1* was strongly RNA dose dependent, whereas I_{basal} of GIRK2 grew much less with channel density (Supplemental Fig. 1*A* and *B*).

The second difference was the effect of coexpression of G$\beta\gamma$. GIRK1* or GIRK2 currents recorded in control and G$\beta\gamma$-expressing oocytes are shown in Fig. 4*E* and *F*, left panels; the right panels show summaries of the experiments of this series. Surprisingly, coexpression of

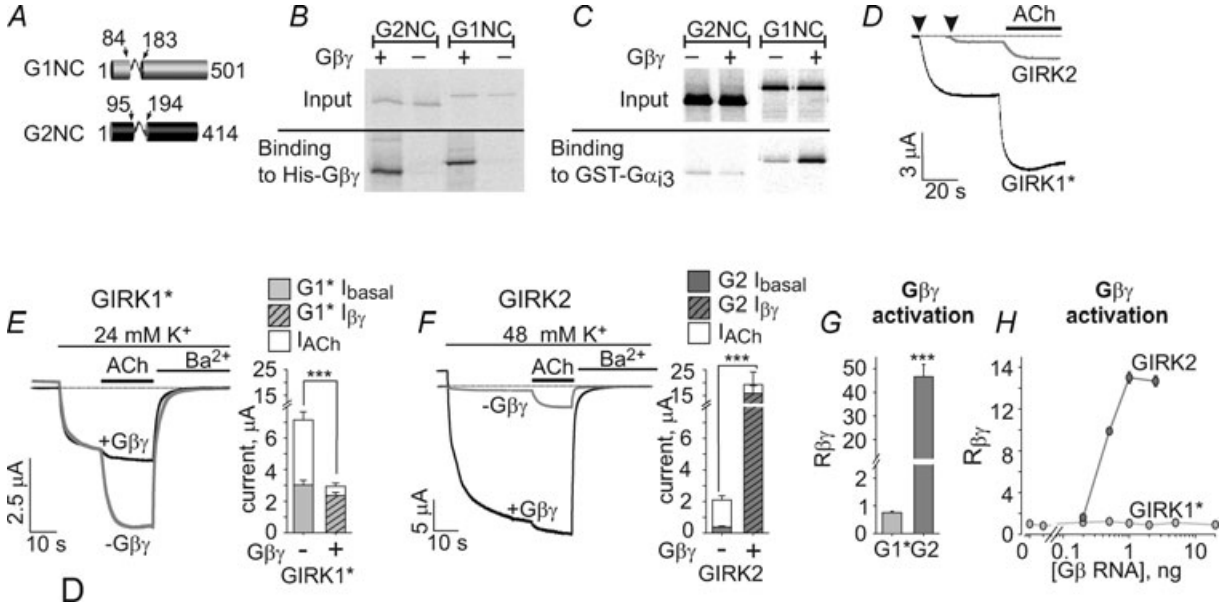

Figure 4. Biochemical and functional differences between GIRK1 and GIRK2
A, schematic representation of the G1NC and G2NC tandems. The transmembrane portion of the channel was replaced by a short linker (shown by a loop connecting the cylinders). *B*, His-G$\beta\gamma$ binds the ^{35}S-labelled, *in vitro* synthesized G1NC and G2NC. Pull down experiments were performed using Ni^{2+} affinity beads. Autoradiograms of loaded (upper panel, 'input'; 1/60 of total loaded protein) and bound ^{35}S-labelled G1NC and G2NC proteins (lower panel, 'binding') are shown. *C*, GST-Gα_{i3} binds G1NC and G2NC. The binding of G1NC, but not G2NC, is enhanced by added purified G$\beta_1\gamma_2$. Pull down experiments were performed using glutathion sepharose affinity beads. These results are representative of 3 independent experiments. *D*, examples of basal and ACh-evoked currents in two representative oocytes expressing homomeric GIRK1* and GIRK2. Arrowheads indicate the exchange of the external solution from low, 2 mM K^+ to high, 24 mM K^+. The addition of 10 μM ACh is indicated by the horizontal bar. *E* and *F*, examples of currents from four different oocytes expressing homomeric GIRK1* (*E*, grey), GIRK2 (*F*, grey) or homomeric channels with coexpression of G$\beta\gamma$ (black traces in *E* and *F*). Holding potential was set to −80 mV. Solutions were switches as indicated. Summaries of the basal, ACh-evoked and G$\beta\gamma$-evoked currents are depicted to the right of the traces in *E* and *F*. GIRK1* is depicted in light grey (*E*) and GIRK2 in dark grey (*F*). In each bar chart, the bottom bar shows I_{basal}, the top open bar shows I_{ACh}, and the total height of each bar represents I_{total}. G1* stands for GIRK1*, G2 for GIRK2. Diagonal strips indicate coexpression of G$\beta\gamma$. $n = 20$–40. *G*, $R_{\beta\gamma}$, the extent of activation by coexpressed G$\beta\gamma$. *H*, titrated expression of G$\beta\gamma$ revealed dose-dependent activation of GIRK2 (one experiment, $n = 5$–6) but no activation of GIRK1* (two experiments, $n = 5$–18). The dose of Gγ was 0.5 of that of Gβ. ***$P < 0.001$.

Table 1. Comparison between GIRK1/2, GIRK1* homomers and GIRK2 homomers

Parameter	GIRK1/2	GIRK1*	GIRK2
I_{basal}	High, $G\beta\gamma$ dependent	High, $G\beta\gamma$ dependent	Low, largely $G\beta\gamma$ independent
Activation by $G\beta\gamma$	Weak or medium at high channel densities ($R_{\beta\gamma}$ 1.4–1.8)	None or negative at high channel densities ($R_{\beta\gamma} \leq 1$)	Strong ($R_{\beta\gamma} > 10$)
$G\alpha_{i3}{}^{GDP}$ on I_{basal}	Decreases I_{basal}	Decreases I_{basal}	Almost no effect
$G\alpha_{i3}{}^{GDP}$ on $R_{\beta\gamma}$	Strong regulation (increases $R_{\beta\gamma}$ with no decrease in $I_{\beta\gamma}$)	Strong regulation (increases $R_{\beta\gamma}$ with no decrease in $I_{\beta\gamma}$)	Weak regulation (no increase in $R_{\beta\gamma}$ and $I_{\beta\gamma}$)
$G\alpha_{i3}$-wt on I_{ACh}	Increases I_{ACh} and R_a with no change in I_{total}	Increases I_{ACh} and R_a with no change in I_{total}	Increases I_{Ach}, R_a and I_{total}

I_{basal} is the agonist-independent basal activity. I_{ACh} is the agonist-evoked response, revealed upon application of ACh via activation of coexpressed m2R. $I_{total} = I_{basal} + I_{ACh}$. $R_{\beta\gamma}$, the relative activation by $G\beta\gamma$, calculated as the ratio of $I_{\beta\gamma}$ measured in a given oocyte which coexpressed $G\beta\gamma$, to the average I_{basal} of the control group lacking coexpressed $G\beta\gamma$ ($R_{\beta\gamma} = I_{\beta\gamma}/I_{basal}$). Note that $I_{\beta\gamma}$ is the total GIRK current, comprising the basal and the $G\beta\gamma$-evoked current. See (Peleg *et al.* 2002; Rubinstein *et al.* 2007) for additional data regarding GIRK1/2.

$G\beta\gamma$ failed to increase whole-cell GIRK1* currents at high channel expression levels (Figs 4*E* and 6*D*), whereas GIRK2 was strongly activated by the coexpressed $G\beta\gamma$ (Figs 4*F* and 8*C*). Titrated $G\beta\gamma$ expression demonstrated a clear dose-dependent activation of GIRK2 by $G\beta\gamma$, which contrasted with lack of activation of GIRK1* by $G\beta\gamma$ at all RNA doses tested (Fig. 4*H*). The differences in the effects of $G\beta\gamma$ were not caused by differential changes in channel expression level (Supplemental Fig. 2). Despite lack of activation of GIRK1*, $G\beta\gamma$ expression almost completely abolished the agonist-evoked response of GIRK1* (Fig. 4*E*). Interestingly, when GIRK1* was expressed at low levels (1–5 ng RNA per oocyte; $I_{basal} < 0.6\mu A$), the coexpressed $G\beta\gamma$ activated the channel ~5-fold (Supplemental Fig. 1*D*), supporting the data reported by (Vivaudou *et al.* 1997). The mechanism of the complex, even paradoxical, behaviour of GIRK1* is still unclear but seems to be connected with its regulation by $G\alpha$ (see below).

Inversely, as mentioned above, GIRK2 was strongly activated by the coexpressed $G\beta\gamma$, as expected from a $G\beta\gamma$ effector (Fig. 4*F* and *H*). $R_{\beta\gamma}$ was 46.6 ± 5.17 (Fig. 4*G*), dramatically higher compared to GIRK1* (0.75 ± 0.05) or even the neuronal GIRK1/2 channel (1.4 ± 0.1, Fig. 2*C*; Table 1). Notably, $I_{\beta\gamma}$ of GIRK2 was ~6-fold higher compared to the total current ($I_{basal} + I_{ACh}$) observed without $G\beta\gamma$ expression (Fig. 4*F*; $16.3 \pm 3.1\ \mu A$ *vs.* $2.6 \pm 0.2\ \mu A$) (see Discussion).

Previously, using the $G\beta\gamma$ scavengers m-phosducin and m-cβARK, we showed that up to 90% of the basal current of the neuronal GIRK1/2 channel is $G\beta\gamma$ dependent (Rishal *et al.* 2005). These two $G\beta\gamma$ scavengers were used to characterize the basal currents of the homomeric channels (Fig. 5 and Supplemental Fig. 3). The PM expression of GIRK1* and especially GIRK2 was substantially reduced by coexpression of m-phosducin (Supplemental Fig. 3), and therefore the currents in Fig. 5 are presented after correction to the relative PM expression. Coexpression of m-phosducin or m-cβARK reduced I_{basal} of GIRK1* by 89–95%, suggesting that the basal activity of GIRK1* is mostly $G\beta\gamma$ dependent, like in GIRK1/2 (see Fig. 2). In contrast, GIRK2 basal activity appeared largely $G\beta\gamma$ independent as its I_{basal} was not inhibited by coexpressed m-cβARK or m-phosducin.

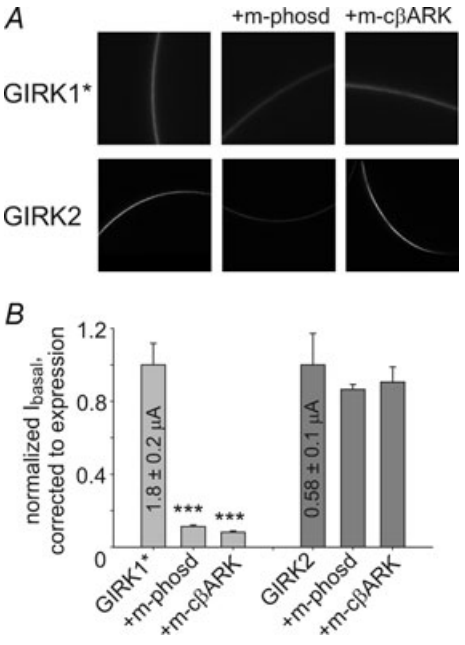

Figure 5. The basal activity is $G\beta\gamma$ dependent in GIRK1*, but $G\beta\gamma$ independent in GIRK2

A, confocal images of whole oocytes expressing YFP-labelled GIRK1* (visualized using YFP) or $GIRK2_{HA}$ (visualized using anti-HA antibody). *B*, the effect coexpression of $G\beta\gamma$ scavengers, m-phosducin (10 ng) and m-cβARK (5 ng), on I_{basal} of GIRK1* (grey) and GIRK2 (dark grey). Currents were corrected to changes in PM level of the channel (shown in Supplemental Fig. 3). $n = 16$–20. ***$P < 0.001$.

GIRK1* is regulated by $G\alpha_{i3}$

The distinct patterns of basal and $G\beta\gamma$-evoked activities in GIRK1* and GIRK2 and the difference in binding of GIRK subunits to $G\alpha_i$ in the presence of $G\beta\gamma$ led us to hypothesize that GIRK1* and GIRK2 may be differentially regulated by $G\alpha_i$. To test this, homomeric GIRK1* channels were coexpressed with $G\alpha_{i3}$-wt, $G\alpha_{i3}$GA or $G\alpha_{i3}$QL, with or without the coexpression of $G\beta\gamma$, and the emerging changes in I_{basal}, I_{ACh}, $I_{\beta\gamma}$, R_a, $R_{\beta\gamma}$ and the channel's surface expression were monitored. Analysis of the effects of $G\alpha_{i3}$ were performed at high GIRK1* expression levels ($I_{basal} > 1.4\ \mu A$) to minimize the potential interference of endogenous $G\alpha_i$ (Peleg *et al.* 2002). GIRK1* PM expression was measured in giant excised PM patches (Singer-Lahat *et al.* 2000; Peleg *et al.* 2002; Kanevsky & Dascal, 2006) (Fig. 6*A*) and found to be largely unaffected by either $G\alpha_{i3}$ variant or by $G\beta\gamma$ (summarized in Fig. 6*B*). Therefore, the recorded whole-cell currents under different treatments were usually compared without correcting them for changes in PM expression.

Coexpression of $G\alpha_{i3}$-wt or $G\alpha_{i3}$GA reduced GIRK1* I_{basal} by 73% or 95%, respectively (see Fig. 6*A* for representative current records, and Fig. 6*Da* for summary), consistent with the observation that GIRK1* I_{basal} is $G\beta\gamma$ dependent, as in GIRK1/2. Also, like in GIRK1/2 (Ivanina *et al.* 2004), coexpression of $G\alpha_{i3}$-wt dramatically increased the relative activation by agonist, R_a (7.6-fold, Fig. 6*C*). In addition, the extent of activation

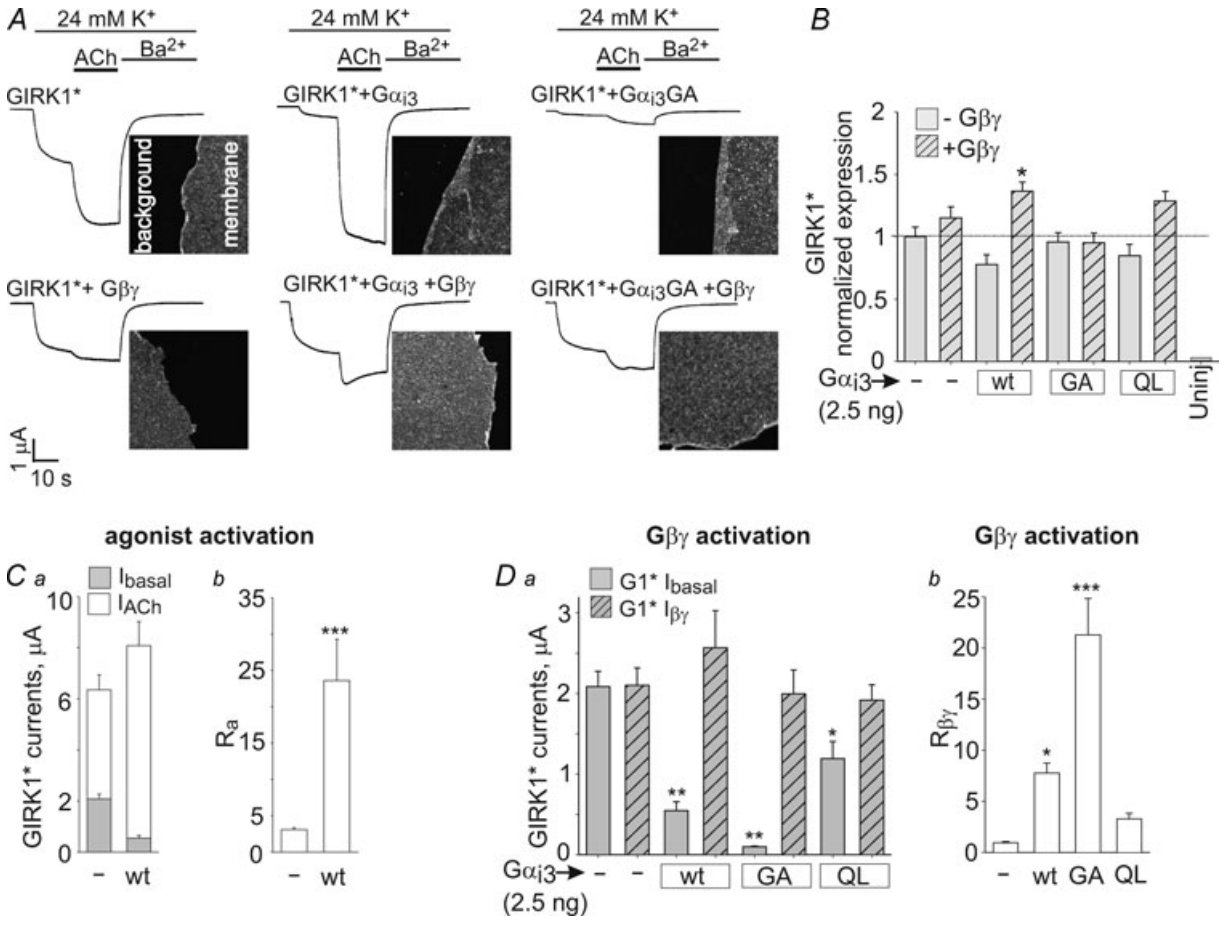

Figure 6. $G\alpha_{i3}$ regulates GIRK1* activation in whole oocytes
A, examples of basal and ACh-evoked currents (continuous lines) of GIRK1* (10–15 ng), with and without coexpression of $G\alpha$ (2.5 ng) and $G\beta\gamma$ (5 and 1 ng RNA, respectively). The images beside the current traces show the PM expression of GIRK1*, monitored in giant excised PM patches using anti-GIRK1 antibody and a secondary, fluorescently labelled antibody. The images focus on the edges of the PM patches to allow comparison with the background. The image area is $55 \times 55\ \mu m$. *B*, summary of GIRK1* expression levels under different conditions. $n = 14$–19. *C*, summary of I_{basal} and I_{ACh} with or without coexpression of $G\alpha_{i3}$-wt (2.5 ng RNA per oocyte) (*a*), and of R_a measured in the same oocytes (*b*). $n = 22$–30. *D*, the effect of coexpression of $G\alpha_{i3}$ (wt, GA or QL, 2.5 ng each) on GIRK1*'s I_{basal} and $I_{\beta\gamma}$ (*a*), and the summary of measurements of $R_{\beta\gamma}$ in this series of experiments (*b*). $n = 17$–36. Statistical comparisons of multiple groups were done using one-way ANOVA followed by Dunnett's test against the control group, GIRK1* alone.*$P < 0.05$; **$P < 0.01$; ***$P < 0.001$.

by Gβγ ($R_{\beta\gamma}$) was greatly increased by $G\alpha_{i3}$: ∼8-fold by $G\alpha_{i3}$-wt (or ∼5-fold if corrected for PM expression changes) and ∼22-fold by $G\alpha_{i3}$GA (Fig. 6*Db*). Neither $G\alpha_{i3}$-wt nor $G\alpha_{i3}$GA reduced $I_{\beta\gamma}$, despite their ability to sequester free Gβγ. Coexpression of $G\alpha_{i3}$QL reduced I_{basal} by ∼40% (Fig. 6*Da*), possibly due to this mutant's ability to bind Gβγ (Majumdar *et al.* 2006); however, $R_{\beta\gamma}$ was not significantly improved by $G\alpha_{i3}$QL (Fig. 6*Db*). Thus, $G\alpha_{i3}{}^{GDP}$ regulates GIRK1* and GIRK1/2 similarly: it decreases I_{basal} and improves $R_{\beta\gamma}$, while preserving $I_{\beta\gamma}$ (Rubinstein *et al.* 2007).

Regulation of GIRK1* by Gβγ and $G\alpha_{i3}$GA was further examined in excised patches (Fig. 7*A*). When oocytes were injected with 10–17 ng of GIRK1* RNA, we observed high cell-to-cell and patch-to-patch variability of channel density (range of I_{basal} in the absence of $G\alpha_{i3}$GA: 0.03–22 pA; Fig. 7*B*), therefore not all patches could be defined as having high channel density (Peleg *et al.* 2002). Nevertheless, GIRK1* showed the main hallmarks of regulation by Gβγ and $G\alpha_{i3}$GA, as in whole cells. (1) Like GIRK1/2, homomeric GIRK1* channels exhibited strong negative correlation between I_{basal} and $R_{\beta\gamma}$ (Fig. 7*B*, left panel, $P < 0.001$), and this correlation was absent in the presence of $G\alpha_{i3}$GA (Fig. 7*B*, right panel). The negative correlation between I_{basal} and $R_{\beta\gamma}$ is an important hallmark of a concerted regulation of I_{basal} by Gα and Gβγ (Peleg *et al.* 2002; Rubinstein *et al.* 2007). (2) $G\alpha_{i3}$GA expression reduced I_{basal} by 70% and improved $R_{\beta\gamma}$ (Fig. 7*C*). (3) The total Gβγ-evoked current was not reduced by $G\alpha_{i3}$GA.

There were, however, quantitative differences with whole-cell data: the average activation of GIRK1* by added Gβγ in excised patches was stronger than by coexpressed Gβγ in whole cells ($R_{\beta\gamma}$ of 12 ± 3.7), and the improvement in $R_{\beta\gamma}$ by $G\alpha_{i3}$GA expression was milder (3-fold). These differences could, at least in part, result from the inclusion in the analysis of low-density patches, which show high $R_{\beta\gamma}$ in the absence of exogenous Gα. Indeed, in seven patches with high I_{basal}, above 2 pA, $R_{\beta\gamma}$ was 1.01 ± 0.27 (range: 0.27–2.04; Fig. 7*B*), resembling the low relative activation of Gβγ in whole cells.

Unfortunately, the same definition of channel density could not be used in cells expressing $G\alpha_{i3}$GA because it strongly reduced I_{basal}. Thus, we attempted to sort out the cells with high expression levels according to high total current, $I_{\beta\gamma}$ (>2 pA). This criterion is applicable to all patches since $I_{\beta\gamma}$ does not depend on the presence of $G\alpha_{i3}$GA (Fig. 7*C*). Under this definition, $R_{\beta\gamma}$ was 5 ± 3 ($n = 10$) in control and significantly higher (44 ± 12, $n = 7$, $P < 0.01$) in $G\alpha_{i3}$GA-expressing cells ($R_{\beta\gamma}$ was 32 ± 8, $n = 12$, in all $G\alpha_{i3}$GA-containing patches). We conclude that $G\alpha_{i3}$GA genuinely improves the relative activation of GIRK1* by Gβγ, as in whole cells. However, in general, activation of GIRK1* by Gβγ in excised patches was better than in whole cells, and therefore an involvement of unidentified cytosolic factors in regulating

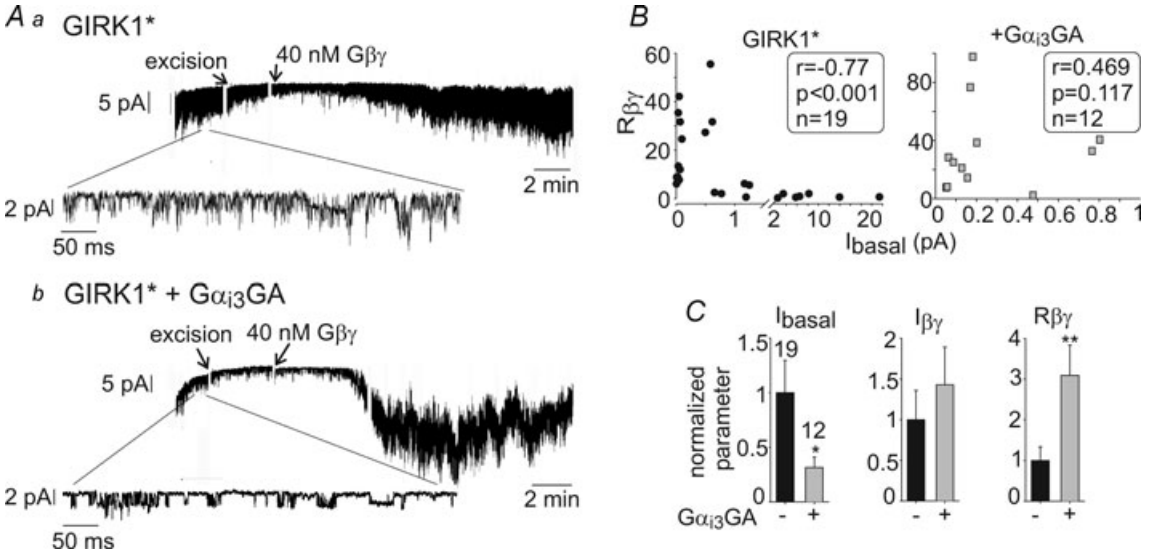

Figure 7. $G\alpha_{i3}$GA regulates GIRK1* in excised plasma membrane patches
GIRK1* (10–17 ng) was expressed with or without $G\alpha_{i3}$GA (2.5 ng). *A*, examples of patch clamp records in oocytes expressing GIRK1* alone (*a*) or GIRK1* with $G\alpha_{i3}$GA (*b*), with zooms on segments of the c.a. records below the main traces. *B*, correlation between I_{basal} (measured in the cell attached mode) and $R_{\beta\gamma}$ with (right) or without (left) $G\alpha_{i3}$GA coexpression. The data were analysed using Spearman's correlation algorithm. Correlation coefficient (*r*), *P* value and *n* are shown in the boxes. *C*, Summary of patch clamp experiments. In view of large batch-to-batch variability, all data (currents, $R_{\beta\gamma}$) were normalized to those of control group (GIRK1* alone) recorded on the same day. The number of measurements is shown on top of the I_{basal} bars (left graph). *$P < 0.05$, **$P < 0.01$.

the G$\beta\gamma$-dependent gating of GIRK1* cannot be ruled out.

GIRK2 is not regulated by $G\alpha_{i3}^{GDP}$

Wild-type GIRK2 channels or $GIRK2_{HA}$ channels containing an extracellular HA tag (Clancy *et al.* 2005) were expressed at 10–15 ng RNA per oocyte with Gα_{i3}-wt, Gα_{i3}GA and Gα_{i3}QL, with or without G$\beta\gamma$. GIRK2 expression was very sensitive to Gα_{i3} and G$\beta\gamma$: coexpression of Gα_{i3}-wt and Gα_{i3}GA reduced PM levels of GIRK2 by up to 80%, while Gα_{i3}QL had a mild effect (Fig. 8*A* and Supplemental Fig. 4*Aa*). Interestingly, coexpression of G$\beta\gamma$ partly restored GIRK2 expression. Thus, PM expression of GIRK2 was monitored in every experiment. GIRK2 and $GIRK2_{HA}$ PM levels were measured by imaging in giant PM patches using anti-GIRK2 antibody, and in intact oocytes with an anti-HA antibody. We compared the two methods for assessment of the relative PM expression of GIRK2 and $GIRK2_{HA}$ under various experimental conditions in the same experiment, and found them to give almost identical results (Fig. 8*A*). These results further validate the notion that the measurements in giant excised PM patches reliably report the surface expression of membrane or membrane-associated proteins (Kanevsky & Dascal, 2006). The results with GIRK2 and $GIRK2_{HA}$ were pooled as there were no substantial differences in PM expression or the effects of Gα_{i3} and G$\beta\gamma$ on channel currents.

After correcting GIRK2 currents for changes in PM expression, we found that I_{basal} was largely unaffected by Gα_{i3}-wt or Gα_{i3}GA (Supplemental Fig. 4*Ab*). $I_{\beta\gamma}$, the total G$\beta\gamma$-evoked current, and $R_{\beta\gamma}$ were also unaffected by coexpression of Gα_{i3} (Fig. 8*B* and Supplemental Fig. 4*Ab*). However, the above correction assumes a linear relation between channel PM levels and whole-cell currents, which may not always hold. Therefore, we also titrated the channel's expression by increasing the amount of injected RNA in order to get equal PM expression with or without Gα_{i3}GA and G$\beta\gamma$ (Fig. 8*C*; see additional details in Supplemental Fig. 4*B*). When groups of oocytes with equal PM expression levels were compared, expression of Gα_{i3}GA only slightly decreased I_{basal} ($P > 0.05$) with no effect on $I_{\beta\gamma}$ or $R_{\beta\gamma}$ (Fig. 8*C*). Thus, $G\alpha_{i3}^{GDP}$ does not alter either basal or G$\beta\gamma$-evoked activity of GIRK2.

In contrast, expression of Gα_{i3}-wt dramatically increased the agonist response (Fig. 8*D*): I_{total} was increased by ∼7-fold and R_a was improved by ∼12-fold (note that R_a is calculated for each oocyte and is therefore independent of the channel expression variations). In this experimental protocol Gα_{i3} serves as the donor of G$\beta\gamma$ following the activation by GPCR. It is plausible that overexpression of Gα_{i3} increases the fraction of GIRK2 channels associated with G$\alpha_i\beta\gamma$ trimers prior to activation, and in effect increased the number of functionally responsive channels (see Discussion). The increase in I_{total} by Gα_{i3}-wt was not observed with GIRK1/2 or GIRK1* (Fig. 6*C* and Ivanina *et al.* 2004).

GIRK2 channels were also tested for activation by purified G$\beta\gamma$ in excised patches. Examples of the currents with or without Gα_{i3}GA are shown in Fig. 9*A*. Unlike GIRK1* (Fig. 7) or GIRK1/2 (Peleg *et al.* 2002), the negative correlation between I_{basal} and $R_{\beta\gamma}$, if any, was weak and did not reach statistical significance either in wt GIRK2 (data not shown) or $GIRK2_{HA}$, with or without Gα_{i3}GA (Fig. 9*B*). Further, in agreement with the whole-cell results, coexpression of Gα_{i3}GA had no effect on GIRK2 I_{basal}, $I_{\beta\gamma}$ or $R_{\beta\gamma}$ (Fig. 9*C*).

In conclusion, although Gα_{i3} binds both GIRK1 and GIRK2 subunits, regulation by $G\alpha_{i3}^{GDP}$ of I_{basal} and of G$\beta\gamma$-induced activation is a unique feature of GIRK1-containing channels.

The C terminus of GIRK1 is important for Gα_i modulation

GIRK1 and GIRK2 differ in sequence and length, especially in the CT, which is ∼320 amino acids long in GIRK1 and only 220 in GIRK2 (see Ivanina *et al.* 2003). The distal CT, starting approximately at amino acid (a.a.) 370 of GIRK1 (381 in GIRK2), is the region of lowest homology between the two subunits. Logothetis and collaborators pointed out the importance of the unique CT of GIRK1 for large currents in the context of a GIRK1/GIRK4 chimera (Chan *et al.* 1997). Accordingly, we hypothesized that this segment may play a role in the unique modulation of GIRK1 by Gα_{i3}. To this end, we constructed a chimeric channel, $G2_{CT}G1$, composed of $GIRK2_{HA}$ in which the distal CT (a.a. 382–414) was replaced with that of GIRK1, a.a. 371–501 (Fig. 10*A*). Monitoring of the PM expression was done in whole oocytes using an external HA tag. Like GIRK1*, the chimeric $G2_{CT}G1$ displayed large basal currents, which were strongly RNA dose dependent, reaching 5.5 μA at 2 ng RNA per oocyte (Fig. 10*C* and Supplemental Fig. 1*C*). On the other hand, coexpression of Gα_{i3}GA reduced the PM expression levels of $G2_{CT}G1$ by ∼60%, resembling in this respect the GIRK2 (Fig. 10*B*). Coexpression of G$\beta\gamma$ induced weak activation with $R_{\beta\gamma}$ of ∼2 and $I_{\beta\gamma}$ of 8.9 μA (or 12.4 μA if corrected to PM expression, Fig. 10*C* and *D*). Gα_{i3}GA coexpression reduced I_{basal} by 96–98% but enabled full activation by G$\beta\gamma$, or even enlargement of the $I_{\beta\gamma}$ if corrected for the reduced expression. $R_{\beta\gamma}$ with Gα_{i3}GA coexpression was increased from 2 to ∼70 (Fig. 10*D*). Therefore, the distal part of GIRK1 CT is important for Gα and G$\beta\gamma$ regulation. Transferring this segment confers upon GIRK2 most (though not all) of the unique qualities of GIRK1*: high, G$\beta\gamma$-dependent basal activity and regulation by Gα_{i3}GA.

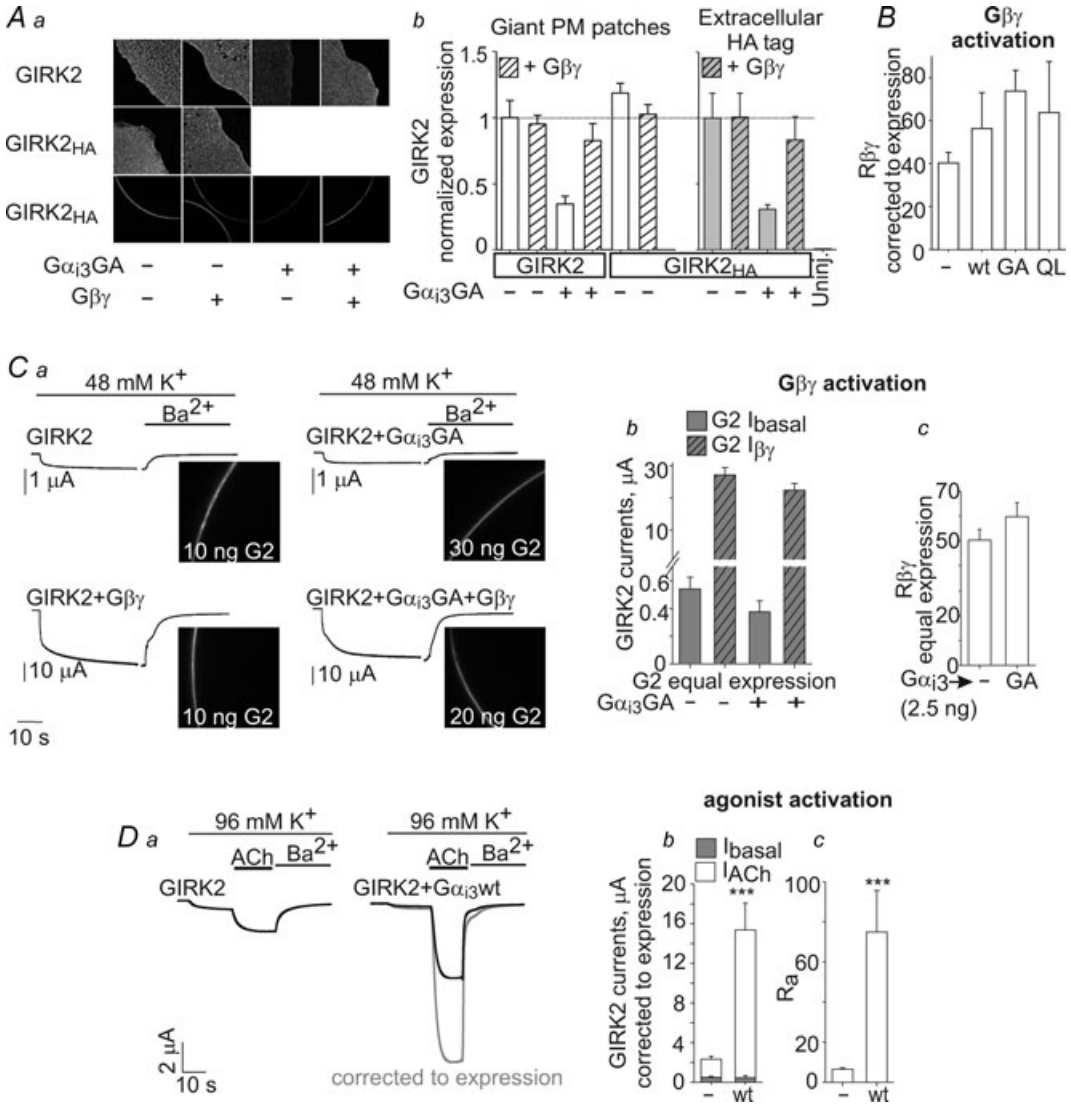

Figure 8. GIRK2 is not regulated by $G\alpha_{i3}$ in whole oocytes

Aa, changes in the amount of GIRK2 channels in PM caused by coexpression of $G\alpha_{i3}$ (2.5 ng RNA) and $G\beta\gamma$ (5 and 1 ng RNA, respectively). Data were obtained by measurements in giant PM patches using anti-GIRK2 antibody and a secondary, fluorescently labelled antibody, or in whole oocytes using external HA tag, in the same experiment. *b*, summary of GIRK2 expression and comparison of the two imaging methods. Open bars show the amount of GIRK2 and $GIRK2_{HA}$ channels, assessed in giant PM patches using the anti-GIRK2 antibody. Grey bars show the PM expression of $GIRK2_{HA}$ measured using the external HA tag. With both methods, the expression level in different groups was normalized to the control group of oocytes expressing the channel alone. Note that both methods provide very similar assessment of the relative effects of expression of $G\alpha_{i3}GA$ (reduction in PM expression levels) and of $G\beta\gamma$ (no change or recovery of expression). $n = 4$–11. *B*, coexpression of $G\alpha_{i3}$ (wt, GA or QL, 2.5 ng each) did not significantly affect $R_{\beta\gamma}$ in a series of experiments where the measured currents were corrected to the PM expression of GIRK2 or $GIRK2_{HA}$ measured in the same experiments. The full details of PM expression, I_{basal} and $I_{\beta\gamma}$ are presented in Supplemental Fig. 4*A*. $n = 13$–28. *C*, summary of a separate experiment in which $GIRK2_{HA}$ PM expression was titrated, by injected different amounts of RNA as indicated on the images, to produce equal channel expression in the presence of coexpressed $G\alpha_{i3}GA$ (2.5 ng) with or without $G\beta\gamma$ (5 and 1 ng RNA, respectively). *a*, the confocal images of whole oocytes obtained with an anti-HA antibody. Examples of currents in representative oocytes are shown to the left of the confocal images. See Supplemental Fig. 4*B* for further details. *b* and *c*, the effect of coexpression of $G\alpha_{i3}GA$ on GIRK2's I_{basal} and $I_{\beta\gamma}$ (*b*) and the summary of measurements of $R_{\beta\gamma}$ (*c*) in groups of oocytes with equal PM channel expression. $n = 8$ oocytes in each group. *D*, examples of GIRK2 currents (*a*) and summaries of I_{basal} and I_{ACh} (*b*) and R_a (*c*) with or without coexpression of $G\alpha_{i3}$-wt (2.5 ng) in four experiments where the amounts of GIRK2 RNA were not titrated, channel expression in the PM was monitored, and current measurements were corrected for PM level changes. $n = 13$–28. $^{***}P < 0.001$.

Discussion

Here we show that $G\alpha_i$ regulates the $G\beta\gamma$ gating of the neuronal GIRK1/2 channels in *Xenopus* oocytes and mammalian (HEK 293) cells. Utilizing 'constitutively inactive' and 'constitutively active' $G\alpha_{i3}$ mutants in functional assays, we find that the 'inactive' $G\alpha_{i3}$ in its GDP-bound form reduces I_{basal} and predisposes GIRK1/2 to $G\beta\gamma$ activation. This action of $G\alpha_i^{GDP}$ is $G\beta\gamma$ dependent and involves the formation of $G\alpha_i\beta\gamma$ heterotrimers. We further explored previously unrecognized differences between GIRK1 and GIRK2 in their interaction with, and functional regulation by, $G\alpha_i$ and $G\beta\gamma$. GIRK1 channels, in contrast to GIRK2 homomers, are regulated by $G\alpha_{i3}$, and consequently show a strikingly different pattern of regulation by $G\beta\gamma$. Our results support the hypothesis that the $G\alpha_{i/o}\beta\gamma$ heterotrimers or free $G\alpha_i^{GDP}$ are regulators of gating of GIRK channels, but potentially limit the list of $G\alpha_{i/o}^{GDP}$-regulated GIRK channels to those containing the GIRK1 subunit.

'Constitutively inactive' mutant of Gα, $G\alpha_{i3}$GA, improves the activation of the neuronal GIRK1/2 by $G\beta\gamma$

We have previously reported that coexpression of $G\alpha_{i3}$-wt reduced the basal activity of GIRK1/2 and enhanced the direct activation of the channels by added $G\beta\gamma$, bypassing the GPCR and the $G\alpha_i\beta\gamma$ heterotrimer dissociation. We initially called this phenomenon 'priming by $G\alpha_i$' and proposed that $G\alpha_i$ regulates GIRK gating, keeping I_{basal} low and preparing the channel for activation by 'free' $G\beta\gamma$ (Peleg *et al.* 2002; Rishal *et al.* 2005; Rubinstein *et al.* 2007). We suggested that GIRK1/2 modulation was mediated by $G\alpha_i^{GDP}$, or $G\alpha_i\beta\gamma$ heterotrimers. Yet, it was also essential to decisively distinguish between effects of $G\alpha_i^{GDP}$ and $G\alpha_i^{GTP}$. *Xenopus* oocytes reportedly contain high basal levels of 'free' $G\beta\gamma$ that help to maintain the meiotic arrest. An unidentified constitutively active GPCR has been hypothesized to cause this condition (Evaul *et al.* 2007), and in such cases a high level of free $G\alpha^{GTP}$ is also expected. Here we showed that only the 'constitutively inactive' mutant $G\alpha_{i3}$GA improves GIRK1/2 activation by $G\beta\gamma$. As with $G\alpha_{i3}$-wt (Rubinstein *et al.* 2007), the improvement is only on the background of a concomitant decrease in basal activity; the total $G\beta\gamma$-induced activation is not changed, both in whole cells and in excised patches. The constitutively active $G\alpha_{i3}$QL did not significantly affect $G\beta\gamma$-induced activation of GIRK1/2 (Figs 2 and 3). However, at present we cannot fully rule out a minor direct effect of $G\alpha_{i3}$QL on GIRK1/2.

Differences in interaction between GIRK subunits and $G\alpha_{i3}\beta\gamma$

Despite a larger $G\beta\gamma$ and $G\alpha$-interacting surface in GIRK1 compared to GIRK2 (Ivanina *et al.* 2003; Ivanina *et al.* 2004), no functional asymmetry was previously reported.

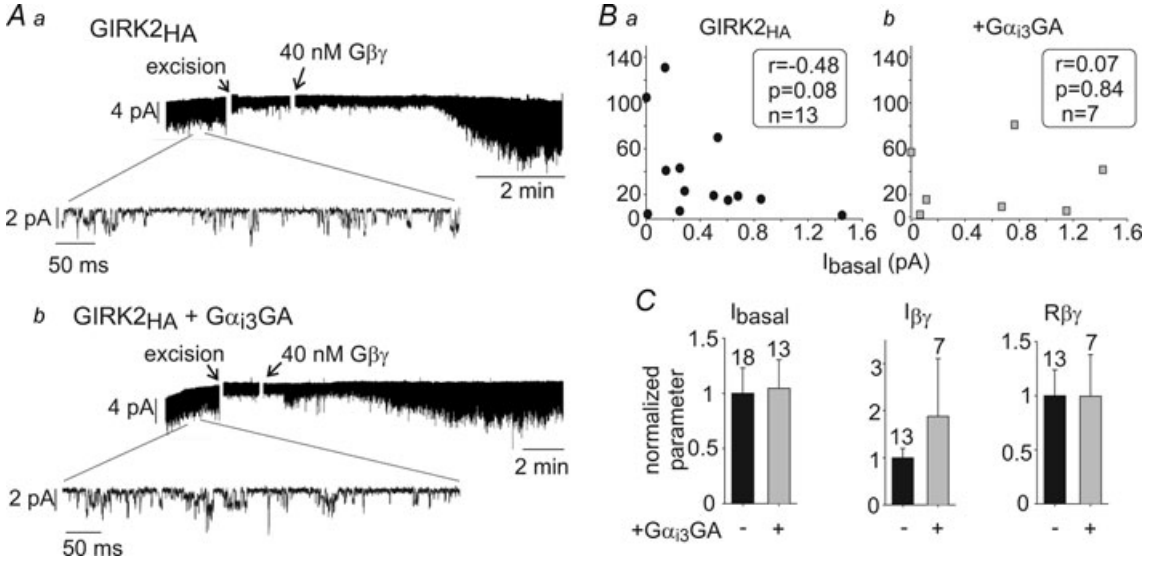

Figure 9. $G\alpha_{i3}$GA does not regulate GIRK2 in excised plasma membrane patches
A, examples of patch clamp records in oocytes expressing $GIRK2_{HA}$ alone (10 ng) (*a*) or $GIRK2_{HA} + G\alpha_{i3}$GA ($G\alpha_{i3}$GA was expressed at 2 ng) (*b*). *B*, correlation between I_{basal} (measured in the cell attached mode) and $R_{\beta\gamma}$ with (right) or without (left) $G\alpha_{i3}$GA coexpression. The data were analysed using Spearman's correlation algorithm. Correlation coefficient (*r*), *P* value and *n* are shown in the boxes. *C*, summary of patch clamp experiments. In view of large batch-to-batch variability, all data (currents, $R_{\beta\gamma}$) were normalized to those of control group ($GIRK2_{HA}$ alone) recorded on the same day. The number of measurements is shown above the bars.

Full cytosolic domains of GIRK1 and GIRK2 interact with $G\beta\gamma$ and $G\alpha_{i3}$. However, regulation (enhancement) by $G\beta\gamma$ of the $G\alpha_{i3}{}^{GDP}$–GIRK interaction is observed only with GIRK1 (Fig. 4). This implies a central role for the GIRK1 subunit in mediating the effects of $G\alpha_i$ (or $G\alpha_i\beta\gamma$) on heterotetrameric GIRK1/2 channels, and possibly on other GIRK1-containing heterotetramers. The enhanced binding of $G\alpha_{i3}{}^{GDP}$ in the presence of $G\beta\gamma$ could be due to stronger binding of $G\alpha_i\beta\gamma$ heterotrimer to GIRK via $G\beta\gamma$, or an enhancement of the direct binding of $G\alpha_{i3}$ to a site separate from that of $G\beta\gamma$. In support, strong binding of $G\alpha_{i1}\beta\gamma$ heterotrimer to the NT of GIRK1 was reported in the past, and this was suggested to reflect the existence of preformed GIRK-G protein signalling complexes (Huang *et al.* 1995).

Homomeric GIRK2 and GIRK1* channels are distinctly regulated by $G\beta\gamma$ and $G\alpha_{i3}{}^{GDP}$

The homomeric GIRK2 channel seems to behave as a 'classical' $G\beta\gamma$ effector, displaying very low basal activity in the absence of agonist and strong activation by added $G\beta\gamma$ (see Table 1). Its gating by $G\beta\gamma$ is not regulated by $G\alpha_{i3}{}^{GDP}$, remaining unaltered in the presence of coexpressed $G\alpha_{i3}$-wt or $G\alpha_{i3}$GA in whole cells or excised patches. In agreement with the biochemical data, several functional results suggest a weak interaction with $G\alpha_i\beta\gamma$ heterotrimers. (1) GIRK2's basal currents are small and insensitive to $G\beta\gamma$ scavengers or to the coexpression of $G\alpha_{i3}$. (2) Coexpression of either $G\alpha_{i3}$-wt or $G\beta\gamma$ enhanced the overall GIRK2 currents (I_{total} and $I_{\beta\gamma}$, respectively) by ~7-fold, compared to control cells expressing the channel alone (Figs 4*F* and 8*D*). Since $G\alpha_{i3}{}^{GDP}$ does not alter the extent of the channel's activation caused by direct addition of $G\beta\gamma$, it is most likely that the addition of $G\alpha_{i3}$ simply increases the amount of $G\alpha_{i3}\beta\gamma$ heterotrimers available for the activation of this channel. These results indicate that the endogenously present $G\alpha_i\beta\gamma$ heterotrimers cannot fully activate all expressed GIRK2 channels, and the majority of GIRK2 homomers (probably more than 80%) lack pre-associated G-proteins (in contrast to GIRK1*, see below). In summary, GIRK2 channels display very strong activation by added $G\beta\gamma$ and no regulation by $G\alpha_{i3}{}^{GDP}$. Lack of regulation of GIRK2 by $G\alpha_{i3}{}^{GDP}$ further emphasizes the authenticity and uniqueness of this regulation in GIRK1-containing channels.

GIRK1* is similar to GIRK1/2 and differs from GIRK2 in two major aspects (Table 1): (1) GIRK1* exhibits a considerable $G\beta\gamma$-dependent basal activity; and (2) it is strongly regulated by $G\alpha_{i3}$. I_{basal} of GIRK1* is highly $G\beta\gamma$ dependent; expression of $G\beta\gamma$-binding proteins m-phosducin, m-cβARK or $G\alpha_{i3}$ reduces I_{basal} by more than 70%. It is highly unlikely that the high I_{basal} of GIRK1* (or GIRK1/2) depends on 'free' $G\beta\gamma$ elevated by some 'constitutively active' GPCR present in the oocyte, because GIRK2 (which is highly sensitive to both $G\beta\gamma$ and ACh) shows almost no $G\beta\gamma$-dependent I_{basal}. Recent studies conducted *in vivo* using fluorescent energy transfer techniques suggest that GIRK1-containing channels are associated with $G\beta\gamma$ both in endoplasmic reticulum (Robitaille *et al.* 2009) and in the PM (Riven *et al.* 2006). Taken together, these considerations suggest that the excessive basal activity of GIRK1* at high expression levels is due to an excess of bound $G\beta\gamma$, and to an insufficient amount of $G\alpha$, as in the case of GIRK1/2 (Peleg *et al.* 2002; Rishal *et al.* 2005).

The data presented here establish that $G\alpha_{i3}{}^{GDP}$, and not $G\alpha_{i3}{}^{GTP}$, is responsible for the regulation of I_{basal} and $R_{\beta\gamma}$ in GIRK1/2 and GIRK1*. Several facts support regulation by $G\alpha_i{}^{GDP}$, probably via the formation of $G\alpha_{i3}\beta\gamma$ heterotrimers. (1) $G\alpha_{i3}$-wt and $G\alpha_{i3}$GA reduced I_{basal} with no reduction in $I_{\beta\gamma}$, and greatly improved the extent of activation by $G\beta\gamma$ ($R_{\beta\gamma}$). (2) In excised patches, $R_{\beta\gamma}$ of GIRK1* exhibited strong negative correlation with I_{basal}, with almost no activation when I_{basal} is high.

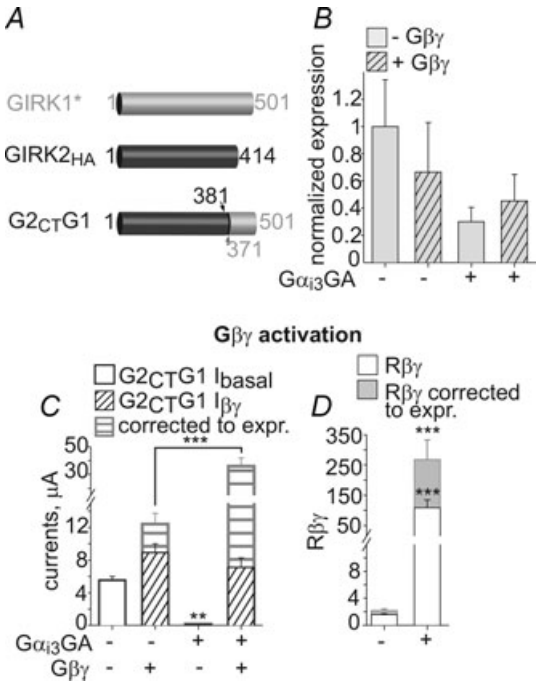

Figure 10. The C terminus of GIRK1 is important for $G\alpha_i$ modulation

A, schematic presentation of the $G2_{CT}G1$ chimera. *B*, summary of $G2_{CT}G1$ expression levels (1–2 ng RNA per oocyte), as measured in whole oocytes using external HA tag. $n = 4$–7. *C*, $G\alpha_{i3}$GA (2.5 ng) regulates I_{basal} and $I_{\beta\gamma}$ of the $G2_{CT}G1$ chimera. Grey bars with horizontal hatching indicate the currents after correction to the PM expression levels (from *B*), diagonal black hatching indicate coexpression of $G\beta\gamma$. *D*, $R_{\beta\gamma}$ with (grey) or without (white) correction to the changes in the PM expression. $n = 7$–24. $^{**}P < 0.05$; $^{***}P < 0.001$.

Expression of $G\alpha_{i3}$GA abolished the negative correlation and improved $R_{\beta\gamma}$ by ∼9-fold. (3) Expression of $G\alpha_{i3}$-wt improved the relative activation by agonist, R_a, by ∼8-fold, but I_{total} did not change. Thus, the improvement of I_{ACh} and R_a correlated with the decrease in I_{basal}, indicating that the expressed $G\alpha_{i3}$ enhanced the amount of GIRK1-associated $G\alpha_{i3}$ and corrected the balance between the bound $G\alpha_{i3}$ and $G\beta\gamma$. Together with the biochemical data, these considerations suggest that most of GIRK1* homomers and GIRK1/2 heterotetramers arrive at the PM in complex with $G\alpha_i\beta\gamma$ or with $G\beta\gamma$ alone.

A plausible model to describe the regulation of GIRK1/2 and GIRK1* by $G\alpha_{i3}{}^{GDP}$ would be one which includes two sites for G protein binding, somewhat similar to the model proposed by Logothetis and colleagues (He *et al.* 1999). In our two-site model the GIRK channel would have a docking, or anchoring, site for $G\alpha_i\beta\gamma$, and a separate activation site that binds $G\beta\gamma$. In a normal physiological situation, $G\alpha_{i/o}\beta\gamma$ is anchored to GIRK either via $G\alpha_i$ (Clancy *et al.* 2005) or via $G\beta\gamma$; the $G\beta\gamma$ activation site is free. Activated GPCR triggers partial or full separation of $G\alpha_{i/o}$ from $G\beta\gamma$, causing a shift of $G\beta\gamma$ to the activation site and opening of the channel. For reasons as yet unclear, the overexpressed channel is trafficked to the PM with excess $G\beta\gamma$ over $G\alpha_{i/o}$ (Rishal *et al.* 2005), and $G\beta\gamma$ is free to interact with the activation site, and hence the high I_{basal}. We further propose that coexpressed $G\alpha_{i3}$ binds $G\beta\gamma$, and the attachment of the resulting $G\alpha_{i3}\beta\gamma$ heterotrimer to the anchoring site reduces the excessive I_{basal} and renders the channel activatable by added $G\beta\gamma$, which can bind to the activation site. In contrast to GIRK1, it appears that GIRK2 does not possess an anchoring site. In a heterotetrameric GIRK1/2, GIRK1 may serve mainly as the $G\alpha_i\beta\gamma$-anchoring subunit and GIRK2 as the $G\beta\gamma$ acceptor responsible for channel activation.

Intricate regulation of gating within the GIRK1–G protein complex

While in general GIRK1* behaved similarly to GIRK1/2 (Table 1), it displayed several features unexpected from a $G\beta\gamma$ effector, which further indicate a complex mechanism of regulation by G protein subunits. The most unique and unexpected feature of GIRK1* homomers is the reduction in the total current upon coexpression of $G\beta\gamma$ (Fig. 4*E*). When the channel was expressed alone, ACh evoked substantial currents. However, $G\beta\gamma$ coexpression failed to activate GIRK1* channels, while completely suppressing the agonist response. The disappearance of I_{ACh} in cells overexpressing $G\beta\gamma$ is observed also with heterotetrameric GIRK1/4 and GIRK1/2 (Reuveny *et al.* 1994; Lim *et al.* 1995; Rubinstein *et al.* 2007) and has been interpreted as indicating full stimulation of GIRK channels by $G\beta\gamma$. This is not the case with GIRK1* (as there is no stimulation). These properties are entirely incompatible with the classical idea of activation of GIRK1* by 'free' $G\beta\gamma$.

Although the molecular mechanisms underlying the peculiar behaviour of GIRK1* are currently unclear, several scenarios based upon the existence of a preformed GIRK1–$G\alpha_i\beta\gamma$ complex seem plausible. GIRK1's CT has been proposed to inhibit channel activation by $G\beta\gamma$ without directly competing with $G\beta\gamma$ for binding to GIRK (Dascal *et al.* 1995; Luchian *et al.* 1997). Such a cytosolic 'lock' may hinder the access of external $G\beta\gamma$ while allowing activation by $G\beta\gamma$ derived from the pre-docked $G\alpha_i\beta\gamma$ heterotrimer. Alternatively (or in addition), $G\alpha_i\beta\gamma$ might allosterically regulate GIRK1* activation, if the proper gating of GIRK1* by $G\beta\gamma$ (via the activation site) requires the docking of $G\alpha_i\beta\gamma$ at the anchoring site. Consequently, overexpression of 'free' $G\beta\gamma$ may deplete the channels of docked $G\alpha_i\beta\gamma$ by sequestering $G\alpha_i$ away from the channel (the 'lock' may allow the exit of pre-docked $G\alpha_i$), weakening the activation by $G\beta\gamma$ when it binds to the activation site. Coexpression of $G\alpha_i$ would correct the gating both by restoring the reserve of docked $G\alpha_i\beta\gamma$, and by regulating I_{basal}. Allosteric interactions between the 'lock', $G\alpha_i$ and $G\beta\gamma$, and the existence of two $G\beta\gamma$-binding sites may produce a complex regulation pattern. Furthermore, additional factors may be involved. We deem it unlikely that the GPCR itself is important in $G\alpha_i{}^{GDP}$-mediated effects, as regulation of GIRK1/2 by $G\alpha_{i3}$ and $G\beta\gamma$ was identical with or without coexpressed GPCRs (Peleg *et al.* 2002; Rubinstein *et al.* 2007). Modulators of $G\alpha$ activity such as Regulators and Activators of G Protein Signaling (RGSs and AGSs, respectively) were proposed to form complexes with and modulate GIRK channels (Jaen & Doupnik, 2006; Wiser *et al.* 2006). Yet, the level of endogenous RGSs in the oocytes is low (Doupnik *et al.* 1997), and titrated coexpression of RGS4 and RGS7 has only marginal effects on I_{basal} of GIRK1/2 (Keren-Raifman *et al.* 2001). A full understanding of the molecular details of regulation of GIRK1-containing channels by $G\alpha$, $G\beta\gamma$ and other factors and the testing of the model proposed above and its alternatives present a challenge for future work.

The unique distal CT of GIRK1 is essential for $G\alpha_{i3}$-dependent regulations

The distal third of the CT of GIRK1 (a.a. 371–501) does not bind $G\alpha_i$ and does not strongly interact with $G\alpha_{i3}$ or $G\beta\gamma$, though it probably possesses a low-affinity $G\beta\gamma$ binding site (Ivanina *et al.* 2003, 2004). Nevertheless, we find that regulation of GIRK1 by $G\alpha_{i3}$ involves this segment of the CT. Its transfer from GIRK1 to GIRK2 conveyed upon GIRK2 most of GIRK1 properties, notably high I_{basal} and strong modulation by $G\alpha_{i3}$GA (a high I_{basal} in a similar GIRK4–GIRK1 chimera has been previously

noted by Chan *et al.* (1997)). These results imply that the end of GIRK1 CT (a.a 371–501) may be important for the anchoring of $G\alpha_i\beta\gamma$ (possibly by interacting with the other parts of the channel rather than with $G\alpha_i\beta\gamma$ itself). Yet, the $G2_{CT}G1$ chimera could still be activated by coexpressed $G\beta\gamma$ (weak activation, $R_{\beta\gamma}$ of $\sim$2), and thus other parts of GIRK1 may be additionally involved in its unique properties. It is also possible that in $G2_{CT}G1$ as well as in GIRK1/2 activation is enabled due to the preservation of $G\beta\gamma$ binding sites of GIRK2, as the latter appears to be an excellent sensor of free 'added' $G\beta\gamma$.

Possible physiological consequences of GIRK1/2 asymmetry

The brain expresses all GIRK subunits, predominantly heterotetrameric GIRK1/2 (hippocampus, cerebellum, cortex), GIRK1/3 and GIRK2/3, and homomeric GIRK2 (substantia nigra) (Koyrakh *et al.* 2005). Variable regional distribution of GIRK2 homomers *vs.* GIRK1/2 implies distinct properties and roles of these channels in different neurons, rendering the discovered differences between GIRK1 and GIRK2 physiologically relevant. We propose that GIRK1-containing channels contribute to the regulation of both basal and neurotransmitter-induced excitability in neurons (indeed, in hippocampal neurons GIRKs were found to contribute to the resting potential; Chen & Johnston, 2005; Wiser *et al.* 2006), whereas GIRK2 homomers serve as a low-noise, high-gain neurotransmitter-induced inhibitory relay.

References

Chan KW, Sui JL, Vivaudou M & Logothetis DE (1996). Control of channel activity through a unique amino acid residue of a G protein-gated inwardly rectifying K^+ channel subunit. *Proc Natl Acad Sci U S A* **93**, 14193–14198.

Chan KW, Sui JL, Vivaudou M & Logothetis DE (1997). Specific regions of heteromeric subunits involved in enhancement of G protein-gated K^+ channel activity. *J Biol Chem* **272**, 6548–6555.

Chen L, Kawano T, Bajic S, Kaziro Y, Itoh H, Art JJ, Nakajima Y & Nakajima S (2002). A glutamate residue at the C terminus regulates activity of inward rectifier K^+ channels: Implication for Andersen's syndrome. *Proc Natl Acad Sci U S A* **99**, 8430–8435.

Chen X & Johnston D (2005). Constitutively active G-protein-gated inwardly rectifying K^+ channels in dendrites of hippocampal CA1 pyramidal neurons. *J Neurosci* **25**, 3787–3792.

Clancy SM, Fowler CE, Finley M, Suen KF, Arrabit C, Berton F, Kosaza T, Casey PJ & Slesinger PA (2005). Pertussis-toxin-sensitive $G\alpha$ subunits selectively bind to C-terminal domain of neuronal GIRK channels: evidence for a heterotrimeric G-protein-channel complex. *Mol Cell Neurosci* **28**, 375–389.

Cruz HG, Ivanova T, Lunn ML, Stoffel M, Slesinger PA & Luscher C (2004). Bi-directional effects of $GABA_B$ receptor agonists on the mesolimbic dopamine system. *Nat Neurosci* **7**, 153–159.

Dascal N (2001). Ion-channel regulation by G proteins. *Trends Endocrinol Metab* **12**, 391–398.

Dascal N, Doupnik CA, Ivanina T, Bausch S, Wang W, Lin C, Garvey J, Chavkin C, Lester HA & Davidson N (1995). Inhibition of function in *Xenopus* oocytes of the inwardly rectifying G- protein-activated atrial K channel (GIRK1) by overexpression of a membrane-attached form of the C-terminal tail. *Proc Natl Acad Sci U S A* **92**, 6758–6762.

Doupnik CA, Davidson N, Lester HA & Kofuji P (1997). RGS proteins reconstitute the rapid gating kinetics of $G\beta\gamma$-activated inwardly rectifying K^+ channels. *Proc Natl Acad Sci U S A* **94**, 10461–10466.

Evanko DS, Thiyagarajan MM & Wedegaertner PB (2000). Interaction with $G\beta\gamma$ is required for membrane targeting and palmitoylation of $G\alpha_s$ and $G\alpha_q$. *J Biol Chem* **275**, 1327–1336.

Evaul K, Jamnongjit M, Bhagavath B & Hammes SR (2007). Testosterone and progesterone rapidly attenuate plasma membrane $G\beta\gamma$-mediated signalling in *Xenopus laevis* oocytes by signalling through classical steroid receptors. *Mol Endocrinol* **21**, 186–196.

Finley M, Arrabit C, Fowler C, Suen KF & Slesinger PA (2004). βL-βM loop in the C-terminal domain of G protein-activated inwardly rectifying K^+ channels is important for $G\beta\gamma$ subunit activation. *J Physiol* **555**, 643–657.

Fishburn CS, Herzmark P, Morales J & Bourne HR (1999). $G\beta\gamma$ and palmitate target newly synthesized $G\alpha_z$ to the plasma membrane. *J Biol Chem* **274**, 18793–18800.

Fowler CE, Aryal P, Suen KF & Slesinger PA (2006). Evidence for association of $GABA_B$ receptors with Kir3 channels and RGS4 proteins. *J Physiol* **580**, 51–65.

He C, Zhang H, Mirshahi T & Logothetis DE (1999). Identification of a potassium channel site that interacts with G protein $\beta\gamma$ subunits to mediate agonist-induced signalling. *J Biol Chem* **274**, 12517–12524.

Hedin KE, Lim NF & Clapham DE (1996). Cloning of a *Xenopus laevis* inwardly rectifying K^+ channel subunit that permits GIRK1 expression of I_{KACh} currents in oocytes. *Neuron* **16**, 423–429.

Huang CL, Jan YN & Jan LY (1997). Binding of the G protein $\beta\gamma$ subunit to multiple regions of G protein-gated inward-rectifying K^+ channels. *FEBS Lett* **405**, 291–298.

Huang CL, Slesinger PA, Casey PJ, Jan YN & Jan LY (1995). Evidence that direct binding of $G\beta\gamma$ to the GIRK1 G protein-gated inwardly rectifying K^+ channel is important for channel activation. *Neuron* **15**, 1133–1143.

Inanobe A, Yoshimoto Y, Horio Y, Morishige KI, Hibino H, Matsumoto S, Tokunaga Y, Maeda T, Hata Y, Takai Y & Kurachi Y (1999). Characterization of G-protein-gated K^+ channels composed of Kir3.2 subunits in dopaminergic neurons of the substantia nigra. *J Neurosci* **19**, 1006–1017.

Ivanina T, Rishal I, Varon D, Mullner C, Frohnwieser-Steinecke B, Schreibmayer W, Dessauer CW & Dascal N (2003). Mapping the $G\beta\gamma$-binding sites in GIRK1 and GIRK2 subunits of the G protein-activated K^+ channel. *J Biol Chem* **278**, 29174–29183.

Ivanina T, Varon D, Peleg S, Rishal I, Porozov Y, Dessauer CW, Keren-Raifman T & Dascal N (2004). $G\alpha_{i1}$ and $G\alpha_{i3}$ differentially interact with, and regulate, the G protein-activated K^+ channel. *J Biol Chem* **279**, 17260–17268.

Jaen C & Doupnik CA (2006). RGS3s and RGS4 differentially associate with GPCR-Kir3 channel signalling complexes revealing 2 modes of RGS modulation: precoupling and collision-coupling. *J Biol Chem* **281**, 34549–34560.

Jelacic TM, Kennedy ME, Wickman K & Clapham DE (2000). Functional and biochemical evidence for G protein-gated inwardly rectifying potassium (GIRK) channels composed of GIRK2 and GIRK3. *J Biol Chem* **275**, 36211–36216.

Kanevsky N & Dascal N (2006). Regulation of maximal open probability is a separable function of $Ca_v\beta$ subunit in L-type Ca^{2+} channel, dependent on NH_2 terminus of α_{1C} ($Ca_v1.2\alpha$). *J Gen Physiol* **128**, 15–36.

Keren-Raifman T, Bera AK, Zveig D, Peleg S, Witherow DS, Slepak VZ & Dascal N (2001). Expression levels of RGS7 and RGS4 proteins determine the mode of regulation of the G protein-activated K^+ channel and control regulation of RGS7 by $G\beta5$. *FEBS Lett* **492**, 20–28.

Koyrakh L, Lujan R, Colon J, Karschin C, Kurachi Y, Karschin A & Wickman K (2005). Molecular and cellular diversity of neuronal G-protein-gated potassium channels. *J Neurosci* **25**, 11468–11478.

Kunkel MT & Peralta EG (1995). Identification of domains conferring G protein regulation on inward rectifier potassium channels. *Cell* **83**, 443–449.

Leaney JL, Milligan G & Tinker A (2000). The G protein α subunit has a key role in determining the specificity of coupling to, but not the activation of, G protein-gated inwardly rectifying K^+ channels. *J Biol Chem* **275**, 921–929.

Lee E, Taussig R & Gilman AG (1992). The G226A mutant of $Gs\alpha$ highlights the requirement for dissociation of G protein subunits. *J Biol Chem* **267**, 1212–1218.

Lim NF, Dascal N, Labarca C, Davidson N & Lester HA (1995). A G protein-gated K channel is activated via $\beta2$-adrenergic receptors and $G\beta\gamma$ subunits in *Xenopus* oocytes. *J Gen Physiol* **105**, 421–439.

Logothetis DE, Kurachi Y, Galper J, Neer EJ & Clapham DE (1987). The $\beta\gamma$ subunits of GTP-binding proteins activate the muscarinic K^+ channel in heart. *Nature* **325**, 321–326.

Luchian T, Dascal N, Dessauer C, Platzer D, Davidson N, Lester HA & Schreibmayer W (1997). A C-terminal peptide of the GIRK1 subunit directly blocks the G protein-activated K^+ channel (GIRK) expressed in *Xenopus* oocytes. *J Physiol* **505**, 13–22.

Luscher C, Jan LY, Stoffel M, Malenka RC & Nicoll RA (1997). G protein-coupled inwardly rectifying K^+ channels (GIRKs) mediate postsynaptic but not presynaptic transmitter actions in hippocampal neurons. *Neuron* **19**, 687–695.

Majumdar S, Ramachandran S & Cerione RA (2006). New insights into the role of conserved, essential residues in the GTP binding/GTP hydrolytic cycle of large G proteins. *J Biol Chem* **281**, 9219–9226.

Masters SB, Miller RT, Chi MH, Chang FH, Beiderman B, Lopez NG & Bourne HR (1989). Mutations in the GTP-binding site of $Gs\alpha$ alter stimulation of adenylyl cyclase. *J Biol Chem* **264**, 15467–15474.

Ogier-Denis E, Houri J-J, Bauvy C & Codogno P (1996). Guanine nucleotide exchange on heterotrimeric Gi3 protein controls autophagic sequestration in HT-29 cells. *J Biol Chem* **271**, 28593–28600.

Peleg S, Varon D, Ivanina T, Dessauer CW & Dascal N (2002). $G\alpha_i$ controls the gating of the G-protein-activated K^+ channel, GIRK. *Neuron* **33**, 87–99.

Rebois RV, Robitaille M, Gales C, Dupre DJ, Baragli A, Trieu P, Ethier N, Bouvier M & Hebert TE (2006). Heterotrimeric G proteins form stable complexes with adenylyl cyclase and Kir3.1 channels in living cells. *J Cell Sci* **119**, 2807–2818.

Reuveny E, Slesinger PA, Inglese J, Morales JM, Iniguez-Lluhi JA, Lefkowitz RJ, Bourne HR, Jan YN & Jan LY (1994). Activation of the cloned muscarinic potassium channel by G protein $\beta\gamma$ subunits. *Nature* **370**, 143–146.

Rishal I, Keren-Raifman T, Yakubovich D, Ivanina T, Dessauer CW, Slepak VZ & Dascal N (2003). Na^+ promotes the dissociation between $G\alpha$-GDP and $G\beta\gamma$, activating G-protein-gated K^+ channels. *J Biol Chem* **278**, 3840–3845.

Rishal I, Porozov Y, Yakubovich D, Varon D & Dascal N (2005). $G\beta\gamma$-dependent and $G\beta\gamma$-independent basal activity of G protein-activated K^+ channels. *J Biol Chem* **280**, 16685–16694.

Riven I, Iwanir S & Reuveny E (2006). GIRK channel activation involves a local rearrangement of a preformed G protein channel complex. *Neuron* **51**, 561–573.

Riven I, Kalmanzon E, Segev L & Reuveny E (2003). Conformational rearrangements associated with the gating of the G protein-coupled potassium channel revealed by FRET microscopy. *Neuron* **38**, 225–235.

Robitaille M, Ramakrishnan N, Baragli A & Hebert TE (2009). Intracellular trafficking and assembly of specific Kir3 channel/G protein complexes. *Cell Signal* **21**, 488–501.

Rubinstein M, Peleg S, Berlin S, Brass D & Dascal N (2007). $G\alpha_{i3}$ primes the G protein-activated K^+ channels for activation by coexpressed $G\beta\gamma$ in intact *Xenopus* oocytes. *J Physiol* **581**, 17–32.

Rusinova R, Mirshahi T & Logothetis DE (2007). Specificity of $G\beta\gamma$ signalling to Kir3 channels depends on the helical domain of pertussis toxin-sensitive $G\alpha$ subunits. *J Biol Chem* **282**, 34019–34030.

Saenz del Burgo L, Cortes R, Mengod G, Zarate J, Echevarria E & Salles J (2008). Distribution and neurochemical characterization of neurons expressing GIRK channels in the rat brain. *J Comp Neurol* **510**, 581–606.

Sharon D, Vorobiov D & Dascal N (1997). Positive and negative coupling of the metabotropic glutamate receptors to a G protein-activated K^+ channel, GIRK, in *Xenopus* oocytes. *J Gen Physiol* **109**, 477–490.

Sheng Y, Tiberi M, Booth RA, Ma C & Liu XJ (2001). Regulation of *Xenopus* oocyte meiosis arrest by G protein $\beta\gamma$ subunits. *Curr Biol* **11**, 405–416.

Singer-Lahat D, Dascal N, Mittelman L, Peleg S & Lotan I (2000). Imaging plasma membrane proteins in large membrane patches of *Xenopus* oocytes. *Pflugers Arch* **440**, 627–633.

Slesinger PA, Patil N, Liao YJ, Jan YN, Jan LY & Cox DR (1996). Functional effects of the mouse weaver mutation on G protein-gated inwardly rectifying K^+ channels. *Neuron* **16**, 321–331.

Slesinger PA, Reuveny E, Jan YN & Jan LY (1995). Identification of structural elements involved in G protein gating of the GIRK1 potassium channel. *Neuron* **15**, 1145–1156.

Torrecilla M, Marker CL, Cintora SC, Stoffel M, Williams JT & Wickman K (2002). G-protein-gated potassium channels containing Kir3.2 and Kir3.3 subunits mediate the acute inhibitory effects of opioids on locus ceruleus neurons. *J Neurosci* **22**, 4328–4334.

Vivaudou M, Chan KW, Sui JL, Jan LY, Reuveny E & Logothetis DE (1997). Probing the G-protein regulation of GIRK1 and GIRK4, the two subunits of the K_{ACh} channel, using functional homomeric mutants. *J Biol Chem* **272**, 31553–31560.

Wickman K & Clapham DE (1995). Ion channel regulation by G proteins. *Physiol Rev* **75**, 865–885.

Wiser O, Qian X, Ehlers M, Ja WW, Roberts RW, Reuveny E, Jan YN & Jan LY (2006). Modulation of basal and receptor-induced GIRK potassium channel activity and neuronal excitability by the mammalian PINS homolog LGN. *Neuron* **50**, 561–573.

Yakubovich D, Rishal I, Dessauer CW & Dascal N (2009). Amplitude histogram-based method of analysis of patch clamp recordings that involve extreme changes in channel activity levels. *J Mol Neurosci* **37**, 201–211.

Yi BA, Lin Y, Jan YN & Jan LY (2001). Yeast screen for constitutively active mutant G protein-activated potassium channels. *Neuron* **29**, 657–667.

Author contributions

N.D., M.R., T.I., S.P., S.B. and C.W.D. conceived the main ideas; N.D., M.R., S.P., T.I., D.B, T.K.-R. and S.B. designed and performed the experiments; M.R. and N.D. wrote the paper; all authors participated in the analysis and interpretation of data, and critically revised and approved the paper.

Acknowledgements

This work is a part of fulfilment of Ph.D. Thesis requirements of S.P., M.R. and S.B. The work was supported by grants from NIH (GM68493 (N.D.) and GM60419 (C.D.)) and the Israel Science Foundation (grants 1396/05 and 49/08 (N.D.)), and a Segol Fellowship from Tel Aviv University Adams Brain Research Center (M.R). We thank Drs D. Logothetis, E. Peralta, E. Reuveny, M. Lohse and P. Slesinger for kindly providing the original cDNAs of human GIRK1*, human m2R, rat m-cβARK (aa 452–689_{end}), bovine phosducin and mouse $GIRK2a_{HA}$, respectively.